Reviewer #1:

We thank the reviewer 1 for the helpful comments and suggestions, which are in plain text below. Our response is in bold text.

A scheme for stream water - aquifer interaction, originally developed by Di et al (2011), was incorporated into CLM model to simulate the influences of river contribution to aquifers through lateral movement of water. Two simulations with and without activating this scheme were run and compared. Based on the model comparisons the importance of taking the surface water – groundwater interactions into consideration for water, energy and carbon balance models was underscored. Overall, the experiments are interesting and adding such a scheme to CLM could potentially improve models accuracy in areas where groundwater surface water interactions exist especially in riparian areas. However, the paper lacks of clarity in presentation. The objectives were not clearly defined and the approach is somewhat obscure. I believe that the most of this paper needs to be rewritten and many additional information need to be supplied before it can be considered for publication.

The model was tested in a single case where river is recharging the groundwater. It would be interesting to see how the model response to the other case such as groundwater recharges to the river. As a matter of fact, this could be the case in the study area, where the original CLM in CTL simulations resulted in depth to groundwater levels about 20 m deeper than the observations. However, it is quite difficult to be sure with the provided groundwater observations data.

Response: Thanks for the comments. As the suggestions, we added some simulations for the case of groundwater recharging river in the sensitivity experiments (page 8, line 28-page 9, line 4; page 9, line 31-page 10, line 18 of the revised manuscript without change tracks), and showed the water table variations in Figure 5.

Also, I would be interested in seeing depth to groundwater level values in TEST and CLM simulation to better understand how groundwater levels respond to lateral water movement from the river as well as how close the groundwater to the surface. Groundwater levels were either given as elevations or difference between CTL and TEST simulations but not in depths. I think giving these values as depths would provide more insight in terms of conceptualize the groundwater interactions with the land surface processes.

Response: Thanks for the comments. As the suggestion, we showed the values of groundwater table depths from CTL, TEST and observation in the Figure 7b, and showed the time series of groundwater table depths from TEST in the Figure 9f-9j. Relevant description and analyses of

the added figures were also settled properly in the manuscript.

Even the critically important model parameters were not provided in the paper. I think that the model parameters and initial conditions as well as how these values were determined need to be explained explicitly. Some of the important parameters including, for example, the soil types and parameters in the simulated stations, the vegetation type and their distributions, the specific vegetation parameters and architecture especially root length density distributions were not provided in the paper. Following the paper is somewhat difficult without knowing the model parameters. A table showing the model input parameters would be quite helpful.

Response: Thanks for the comments. As the suggestion, we made a table (table 2 of the manuscript) to show soil type and vegetation type over both sides of the selected five sections, and explained more clearly about how we got the initial conditions (page 9, lines 25-28). To other model parameters, such as the parameters related to atmospheric boundary layer, hydrology, thermodynamics and vegetation (including root length density), the default settings of CLM4.5 were applied. Detailed information about these parameters could be found in the technical description of CLM4.5 (Oleson et al. 2013). The description above was added in the manuscript (page 9, lines 13-20).

Two sets of sensitivity simulations were run. The first one was used to investigate the model responses to river stages and the second one to river bed hydraulic conductivity. In the second sensitivity simulations, it was found that the model results are not sensitive to the hydraulic conductivity of the river bed (Kr). Theoretically, Kr is a parameter that controls the water transfer between the river and the aquifer besides the head difference between them. However, the reason why the model is not sensitive to the Kr was not discussed in the paper. I think this is important to know and the reason should be discussed in detail and if necessary the additional simulations should be conducted to test if it is a problem related to the numerical scheme or the structure of the model.

Response: Thanks for the comments. In fact, the water table is sensitive to the river bed water conductivity *Kr* in the short-term simulation, while in the long-term simulation the effect of river bed water conductivity is not such significant. To demonstrate this, we plotted the results of short-term (7 days) and long-term (160 days) simulations in Figure 4 and Figure 5. It can be seen that from Figure 4i-4l: As the *Kr* ranged from 3 m d^{-1} to 24 m d^{-1}, the time spent by the nearest grid (to river) to get the equilibrium state is shortened from 2 days to 0.5 days. However, after long-term simulation (Figure 4m-4p), the groundwater table depths are similar for all values of *Kr*. This is because, river bed water conductivity *Kr* only connects the river and the nearest model grid (to the river), while the rest of grids (not next to river) are not directly

influenced by *Kr* and are more affected by the lateral hydraulic conductivity *K* of the riverbank soil (in Eq. (9)). The discussion above were added in the manuscript (page 9, line 31-page 10, line 18) to make the results clearer.

An eddy covariance (EC) station was used to validate the model findings. However, some additional information about the station need to be given. For example, the exact location of the station should be placed in Fig. 3. Also, its fetch area needs to be described with the vegetation information. Moreover, EC data were only compared with TEST simulations. I think including the CTL simulations to the same plot would show how the model results improved by adding the stream-aquifer interaction scheme to the model.

Response: Thanks for the comments. As the suggestions, the exact location of the station was placed in the Figure 3, and the results from CTL simulation were added to the Figure 5 to show the improvement of our model. The land cover was also introduced in the manuscript (page 10, lines 26-27).

In Fig. 7, simulated surface temperature was compared with remotely sensed temperature values. The heat transfer algorithm used in the model can be briefly explained because it would be helpful to understand how the shallower groundwater could alter the surface temperature. Also, I would be curios about to know how the boundary conditions were set up, and how the temperature of the river was treated, used as model forcing or a constant temperature was assigned. Again, I think CTL simulations needs to be included in Fig. 7 as well to show the degree of improvement of the model results.

Response: Thanks for the comments. As the suggestions, we gave a brief introduction of the heat transfer algorithm (including the boundary condition) of CLM (page 7, lines 9-26) and explained why the temperature was affected by the stream-aquifer water interaction. Currently, the river temperature and the horizontal heat transfer are not included, but will be incorporated to our model in the future. The CTL simulations were added in Figure 8 to show the degree of improvement of the model results.

Some specific comments:

1) Abstract could be improved by adding a conclusion sentence. Also, it reads as no validation available in the paper.

Response: Thanks for the comments. We have added the sentences about the model validation

(page 1, lines 15-16) and conclusions (page 1, lines 26-27) as suggestions.

2) Introduction part is quite brief and lack of objectives of the paper, which needs to be clearly stated.

Response: Thanks for the comments. We have enriched the introduction (page 1, line 29-page 2, line 3) and added the objectives of the manuscript (page 2, lines 29-33) as the suggestions.

3) Model time step definitions should be consistent. Please use either 1800s or 0.5h.

Response: Thanks for the comments. We unified the time step to 1800 s in the manuscript.

4) The title of section 4.2 is identical with the title of section 4, please add titles properly as necessary.

Response: Thanks for the comments. We changed the title of section 4 to "Results".

5) Figures are usually not well presented and explained. For example:
(a) Figure 1c: what the lengths of the boxes represents is not clear. Are these grid cells as described in the caption or they are water heads?

Response: Thanks for the comments. We have modified the figure based on the suggestion. The dash lines represent the water heads in the new revised figure.

(b) Figure 4: why and how 20 grid cells were used was not explained.

Response: Thanks for the comments. We plotted water tables of all the grid cells in the revised Figure 4 and Figure 5 instead of showing only 20 grids.

(c) Figure 5, 7: please add CTL simulation results.

Response: Thanks for the comments. We have added the CTL simulation results to these figures as the suggestion.

(d) Figures 12 to 16: the reason why the left and right sides of the river channel are not symmetrical is not clear. Is it due to the soil type or vegetation? Please clearly provide their distributions.

Response: Thanks for the comments. The asymmetrical effects was mainly produced by the

asymmetrical topography. We plotted the terrain elevations of both sides of the 5 sections in Figure 13 and gave an explanation for the asymmetric effects (page 14, lines 9-16).

Reviewer #2:

We thank the reviewer 2 for the helpful comments and suggestions, which are in plain text below. Our response is in bold text.

Title: Eco-hydrological effects of stream-aquifer water interaction: A case study of the Heihe River Basin, northwestern China Authors: Zeng et al.

Summary: This work presents the impact of river network-aquifer interaction on both sides of the river network using 1D lateral groundwater model. On both sides of the river network groundwater exchange is simulated over a region of 3 km using a pixel resolution of 60 m. For each pixel the vertical column response is simulated using the CLM4.5 model. Results show that the river network has an impact on the saturated and unsaturated zone dynamics in close vicinity of the river network. These variations have an impact on the water, energy and ecological properties of these grid cell.

Overall quality: Reading the title and abstract of this manuscript I was quite enthusiastic about the content of this work. However, after thoroughly reading the rest of this work I ended up feeling rather disappointed. The authors basically show that incorporating river-groundwater interactions has an impact on the water table and unsaturated zone dynamics. And these variations have impact on the carbon and energy fluxes. As such, the message presented in the abstract does not correspond well with the content of the manuscript. In my comments below I have tried to provide some more detailed information on how to improve this discrepancy. Furthermore, I need to stress the important equations as given by Eqs. 6-8 seem mathematically incorrect (see below). I would like to ask the authors to make sure that these are just typos and that the model was correctly implemented. If this is not the case, the simulations performed in this work need to be redone. That being said, the overall results presented in this work are fine and fit within the scope of HESS. Therefore, in its current form I recommend major changes. These changes are mainly related to the textual content of the manuscript.

General comments:

1) Page 1, lines 15-16 and page 16, line 1 states that stream aquifer interaction processes were incorporated into CLM4.5. I do not agree with this statement. From what I understand from the modelling set up, based on reading the paper, the authors have simulated the hydrological response of 50 pixels of each 60 m wide on both sides of the river and simulated the vertical response of each pixel using CLM 4.5. Furthermore, the response of the river network is not explicitly simulated using CLM4.5 but is externally forced in the model. In the current version for of the manuscript, the authors give the impression as if a major addition was added to the model. I do not believe that this the case

while reading the paper. The authors only present 1 dimensional lateral groundwater exchange model, which obtains its water level estimate from CLM4.5.

Response: Thanks for the comments. As the suggestion, we changed the way of expression from "incorporating stream-aquifer interaction scheme to CLM and model development" to "combining the two models to investigate the effects of stream-aquifer water interaction" in the abstract, introduction and throughout the manuscript.

In fact, the two models are two-way coupled. That means, besides the presenting of one-dimensional lateral groundwater exchange model which obtains its water level (and some other parameters) estimate from CLM4.5, we also modified the simulated groundwater table and aquifer water storage of CLM4.5 based on the output of the lateral groundwater exchange model. We took advantages of both the models. It is not a major modification to CLM but can be seen as a convenient and effective way to achieve our scientific goals.

2) Page 4, lines 11. Generally CLM4.5 is use for large-scale simulation (global/continental) using relatively coarse grid resolution (about 0.1-1 degree). Furthermore, these simulations usually make use of a 2D lateral grid structure, even though the official version of CLM4.5 does not explicitly represent lateral groundwater flow, but instead the lateral groundwater flux (as estimated using a non-linear reservoir model) is directly moved into the river network. Given this difference in the official version set up and the set up used here (see also previous point) I would suggest to add a section between 2.1 and 2.2 which shows the 1D lateral grid set up up (on both sides of the river network using a high pixel resolution) used here. This will really help improve the readability of the manuscript. E.g. it will then become much easier to understand page 4, lines 9-18.

Response: Thanks for the comments. As the suggestion, we added a section of "Configuration of CLM4.5 for simulation over riverbank" (page 3, line 18-page 4, line 6 of the revised manuscript without change tracks) to introduce how we set up the model and prepared the surface dataset which is the most important in riverbank simulation. Furthermore, the subsurface runoff scheme in CLM4.5 was turned off because it was not suitable in the fine-scale modeling and replaced by the groundwater lateral flow in stream-aquifer interaction scheme, which was the explicit representation of the subsurface process (page 4, lines 2-6).

3) Page 3-4, Eqs. 1-4. The authors present here presents the 1-dimensional lateral groundwater flow equation here with a flexible downstream head boundary condition (i.e. the river network). This model is used to simulated the groundwater response on CLM. In the original version of CLM4.5 a non-linear groundwater reservoir model is used. However, in the manuscript no information is provided, whether this original model was removed in the setup of the authors? Please provide some

additional details here (see also comments below).

Response: Thanks for the comments. The flexible downstream head boundary condition was only used when running the stream-aquifer water interaction module and did not directly connect to CLM4.5. All the vertical biogeophysical and biogeochemical processes of CLM4.5 was retained because they were not scale-dependent and could be used in any resolution if the corresponding surface dataset was set properly. To the non-linear groundwater reservoir model of original CLM4.5, the vertical water exchange scheme between soil and aquifer was not modified. However, as referred above, the subsurface runoff of the original CLM4.5 was turned off in the model because it was not fit for the fine-scale modeling and was replaced by our lateral groundwater exchange model. The Relevant discussions were added in the new section 2.2 of "Configuration of CLM4.5 for simulation over riverbank" in the manuscript (page 3, line 18-page 4, line 6).

4) Page 5, line 6 Change "i.e. water : : : 3.8m" to "i.e. water table lies within 3.8m from surface."

Response: Thanks for the comments. We modified the sentence as the suggestion.

5) Page 5, Eq. 6. There is know information provided on what T1 and T2 indicate?

Response: Thanks for the comments. We added related information about T_1 and T_2 in the appropriate position (page 5, lines 17-18).

6) Page 5, Eq. 7. Mathematically this is incorrect as the transmissivity is obtained from the groundwater level up to the depth of the bedrock. The summation should therefore not include all 10 layers. Instead if the groundwater level lies within layer i: (z_wt – z_(i,bot))*K_i + summation from layer j=i+1 till layer j=10 of (delta z_j*K_j). Where z_wt is the depth of the groundwater table (Eq. 5) and z_(i,bot) is the bottom level of layer i.

Response: Thanks for the comments. We are sorry for this mistake and corrected it in the manuscript (page 5, line 15). We ensure that it is only a slip of typing. The model code is correct.

7) Page 5, Eq. 8. After this equation please add: "where, z' = z-3.8.

Response: Thanks for the comments. We added the sentence as the suggestion.

8) Page 8, line 4-5. The manuscript states that an initial spin-up of 700 years was conducted using the

original CLM4.5 model. So without groundwater exchange. This looks very impressive but seems very redundant as well. Given the resolution of the CLDAS dataset (0.0625 degrees corresponding to 7.5km), means that all 50 cells on each side of the river receive the same type of input. Without accounting for lateral exchange, basically means that they all give the same results, indicating that the simulations can be performed using a single pixel. I cannot believe that one needs 700 years of spin-up simulations to reach some kind of equilibrium groundwater level. Please provide more information here why this was performed.

Response: Thanks for the comments. Although the resolution of atmospheric forcing dataset is coarse, the topographic, land cover, soil datasets for making CLM surface dataset are fine (ASTER Dem Dataset with 30-m, MICLCover with 1-km, HiWATER Land Cover Map with 30-m and China Soil Characteristics Dataset with 1-km). So we think it is necessary for the spin-up over all grids. The choice of 700 "spin-up" years was based on the user's guide of CLM (Chapter 4 of Kluzek 2013) showing that when the biogeochemistry carbon-nitrogen module of CLM is turned on (it is the case of this study), the model should be at least run for 700 years to get a steady state because the magnitudes of carbon and nitrogen fluxes are very small (Oleson et al. 2013). The discussion above was added in the manuscript (page 8, lines 25-28; page 9, lines 13-20).

9) Page 8, line 15. Please add a line indicating that for the river cell in the middle, no simulations with CLM4.5 were performed. But instead a boundary condition was enforced here.

Response: Thanks for the comments. We added the sentence as the suggestion.

10) Page 8, lines 12-20. For each of the 50 pixels on both sides of the channel network, did the authors consider elevation variations between the pixels?

Response: Thanks for the comments. Certainly we took the elevation variations into consideration, for it is the major control of the groundwater lateral flow. We got the high-resolution elevation data from ASTER Dem Dataset with 30-m resolution.

11) Page 8, lines 12-20. It is not clear how the control simulations where implemented? Lines 13-15 state the these do not take stream-aquifer interaction into account. It is not clear whether these simulations do account for lateral groundwater exchange (Eq. 1-4) and how groundwater is removed into the river network (was there some additional boundary condition used?). The results in this manuscript show that there are considerable differences between the CTL and TEST simulations. However, as the current manuscript does not provide much info on how CTL was implemented, it is

currently unknown whether how important these difference are (or whether is it just related to the set up of the model).

Response: Thanks for the comments. The control simulations took the groundwater lateral flow into account because in this study we focused on the effects of stream-aquifer water interaction, but not the groundwater lateral flow. The only difference of CTL from TEST is that the water exchange between stream and aquifer was set to zero (flexible boundary condition). We added this information into the manuscript (page 9, lines 7-9).

12) Page 8, line 19. What is the resolution of the MICLCover land cover map used here?

Response: Thanks for the comments. The resolution of MICLCover land cover is 1-km. The divide of land cover types of MICLCover is similar to CLM. However we also referred the HiWATER Land Cover Map (30-m resolution) when making the surface dataset. We added this information in the manuscript (page 9, lines 13-20).

13) Page 8-9, sensitivity experiment 1 and 2. On page 9, lines 12-13 it is mention that the groundwater table variations are not sensitive to k_r. By directly comparing the chosen values of k_r with those of the saturated lateral hydraulic conductivity value of the surrounding soils Ksoil, one could already made a first impression whether this would have a impact. In case k_r is much larger than Ksoil (as I expect to be the case here), I do not see a reason why to perform this experiment. As these results were to be expected. Therefore, I would remove these results from the manuscript (this will also reduce the number of figures presented in this work, which is rather large).

Response: Thanks for the comments. It is right that *k_r* is several times larger than *Ksoil*. However, the *k_r* is still matter when the simulation time is short. To show this (as well as to meet the comments from another reviewer), we added the results from short-term (7 days) sensitivity experiments in the Figure 4a-4d and 4i-4l. They revealed that the river bed water conductivity is more important in the controlling of short-term water table variation than the controlling of long-term water table equilibrium. The discussion was added in the manuscript (page 9, line 31-page 10, line 18).

14) Page 9, lines 1-2. See comment #8.

Response: Thanks for the comments. The reason of 700 years spin-up was explained in the response to comment #8.

15) Page 10, lines 1-3. In my opinion these results just show that the model correctly adjust to changes in the observed surface temperature.

Response: Thanks for the comments. As the suggestion, we changed the sentence of the explanation for Figure 6a.

16) Page 10, line 6. Change "good ability" to "reasonable ability".

Response: Thanks for the comments. We changed the words as the suggestion.

17) Page 10, lines 9-18 and Fig. 6. The results presented in this figure are heavily depend on the local surface elevation enforced in the model. I would therefore suggest the rescale and plot the difference as with respect to the local surface elevation (yaxes) as function of distance from the channel network (x-axis). This helps to improve the interpretation of this figure.

Response: Thanks for the comments. We plotted the figure (Figure 7c) as the review's suggestion over the Gaotai Bridge where most water wells were displayed.

18) Fig. 7. Note that the legend is a dashed line, while this is not shown in any of the panels.

Response: Thanks for the comments. We modified the Figure 8 to make it clearer.

19) Page 10, lines 17-18. Please mention that the quality of these results are directly influenced by the chosen saturated hydraulic conductivity values, which in this study were chosen a priori and as such not optimized in any kind of manner.

Response: Thanks for the comments. As the suggestion, we added this statement in the manuscript (page 11, lines 20-22).

20) Page 12, line 1. Please add ", see Section 4.2.2." after "from a stream".

Response: Thanks for the comments. As the suggestion, we changed the words as the suggestion.

21) Page 17, lines 14-15. Please remove this statement from the manuscript. This work presents a theoretical study using an extremely high pixel resolution in the direction perpendicular to the river network. Such, resolutions at large scale are infeasible. Even if this would be possible, such an implementation would need many additional model changes not accounted for in the model set up

presented in this work.

Response: Thanks for the comments. We deleted these statements as the suggestion. Maybe in the future we can summarize the findings over the high resolution pixels and come up with some parameterizations to make CLM being able to simulate the effects of stream-aquifer water interaction over large-scale. Thank you!

Eco-hydrological effects of stream-aquifer water interaction: A case study of the Heihe River Basin, northwestern China

Yujin Zeng[1, 2], Zhenghui Xie[1], Yan Yu[3], Shuang Liu[1, 2], Linying Wang[1, 2], Binghao Jia[1], Peihua Qin[1], Yaning Chen[4]

[1]State Key Laboratory of Numerical Modeling for Atmospheric Sciences and Geophysical Fluid Dynamics, Institute of Atmospheric Physics, Chinese Academy of Sciences, Beijing, 100029, China
[2]College of Earth Science, University of Chinese Academy of Sciences, Beijing 100049, China
[3]Zhejiang Institute of Meteorological Sciences, Hangzhou, 310008, China
[4]Key Laboratory of Oasis Ecology and Desert Environment, Xinjiang Institute of Ecology and Geography, Chinese Academy of Sciences, Urumqi, 830011, China

Correspondence to: Zhenghui Xie (zxie@lasg.iap.ac.cn)

Abstract. A scheme describing the process of stream-aquifer interaction wasand the land model CLM4.5 werewas combined with the land model CLM4.5applied incorporated into the land model CLM4.5 to investigateinvestigate the effects of stream water conveyance over riparian banks on ecological and hydrological processes. Two groups of simulations for five typical river cross-sections in the middle reaches of the arid zone Heihe River Basin were conducted. The comparisons between the simulated results and the measurements from water wells, fluxnet station and remote sensing data showed good performance good skills of the coupled model. The simulated riparian groundwater table at a propagation distance of less than 1 km followed the intra-annual fluctuation of the river water level, and the correlation was excellent (R^2 = 0.9) between the river water level and the groundwater table at the distance 60 m from the river. The correlation rapidly decreased as distance increased. In response to the variability of the water table, soil moisture at deep layers also followed the variation of river water level all year, while soil moisture at the surface layer was more sensitive to the river water level in the drought season than in the wet season. With increased soil moisture, the average gross primary productivity and respiration of riparian vegetation within 300 m from the river at a typical section of the river increased by approximately 0.03 mg C m^{-2} s^{-1} and 0.02 mg C m^{-2} s^{-1}, respectively, in the growing season. Consequently, the net ecosystem exchange increased by approximately 0.01 mg C m^{-2} s^{-1}, and the evapotranspiration increased by approximately 3 mm d^{-1}. Furthermore, the length

of the growing season of riparian vegetation also increased by 2–3 months due to the sustaining water recharge from the river.– Overall, the stream-aquifer water interaction plays an essential role in the controlling of riparian hydrological and ecological processes..

1 Introduction

Water is indispensable for human society and eco-hydrological system (Milly et al. 2005; Ouyang et al. 2003; Shen and; Chen 2010; Zhao and; Cheng 2002). Among variety kinds of water resources, aquifer water and stream water, which constitute more than 30% of the freshwater storage, are key factors in hydrological cycle (Chen and; Xie 2010; Schä et al. 1999; Xie et al. 2014; Yu et al. 2014). The aquifer water usually , with its table spatiotemporal fluctuations, acts as a water buffer reservoir to the ecological and hydrological system (Fan 2015; Tsur and; Graham-Tomasi 1991). From the perspective of time, unconfined aquifer stores water resource by plenty recharge from soil infiltration and precipitation Iin humid season, aquifer water can store the excess rainfall, and in arid season, it reversely recharges discharges water theto wet root-zone soil and sustains the ecosystem above by upwards capillary flux (Nepstad et al. 1994). The stream is also very important in the eco-hydrological system. It From the perspective of space, the aquifer water lateral flow continuously transports water from humid or ridge regions to arid or valley regions and supports the ecosystem in the lower-reach area (Contreras et al. 2011; Jobbagy et al. 2011). If considering the topography and river network distribution from catchment scale, water interaction between aquifer and river stream is an essential factor to explain the pattern of groundwater table level, soil moisture, evapotranspiration, water balances, vegetation types and status, and even micro-scale climate along with the river bank (Constantz 1998; Lehr et al. 2015; McNamara et al. 2005). In wet region or season, rainfall or snow melting can uplift groundwater table head, make it higher than vicinal river level and sustain base flow (Arnold et al. 2000). While in arid region or season when river level is higher than local groundwater table head, channel water, which is conveyed from upstream areas, will be transmitted from river to unconfined aquifer in the downstream areas by lateral discharge (Scanlon et al. 2002). This process is the key factor to maintain the riparian ecosystem over arid and semi-arid areas and that is why we can see lush forests line the river corridors but shrubs and grasses cover the plateaus (Sheldon et al. 2010). If we decide to implement some measures (e.g. artificial water conveyance) to maintain the subsistence of the

~~riparian ecosystems adapting to climate change and heavier human water withdraw over arid or semi-arid regions where vegetation growths in these regions depend on the water transported from river lateral recharge rather than precipitation, to understand and quantify this effects of the water interaction between stream and unconfined aquifer could not be more important (Baskaran et al. 2009).~~

The relationship between w~~W~~ater in streams and aquifers are close ~~closely related~~ and both resources have important roles in the carbon-water cycle and in supplying human needs (Chen and Xie, 2010, 2012; Yu et al., 2014; Zou et al., 2014, 2015; Xie et al., 2014). In a wet region, rainfall or melting snow can raise the groundwater table to an elevation higher than that of the vicinal stream level, and~~;~~ groundwater can ~~also~~ sustain~~s~~ base flow in streams and rivers (Arnold et al., 2000). In an arid region, groundwater is recharged laterally from rivers to unconfined aquifers by the stream water conveyance, which sustains the terrestrial ecosystem along the natural channel (Scanlon et al., 2002; Chen et al., 2004, 2010) and induces an increase of riparian soil moisture, soil evaporation, and vegetation transpiration. The growth of riparian vegetation and subsequently changes in carbon cycle processes respond to the water supplement of streams. Understanding and quantifying the effects of stream water conveyance over riparian banks on ecological-hydrological processes is of significance for water resources management (Baskaran et al., 2009).

To investigate the interaction between groundwater and climate, Liang et al. (2003) and Liang and Xie (2003) presented a new parameterization to represent surface and groundwater dynamics and implemented it into the variable infiltration capacity model. Studies have documented that the interaction between surface water and groundwater significantly affect the partition of the water budget and then the land-atmosphere interaction (Maxwell et al., 2007; Maxwell and Kollet, 2008; Fan and Miguez-Macho, 2010, 2011; Fan et al., 2015). To predict the water table elevation near a river channel in an arid region from river discharge, Xie and Yuan (2010) developed a statistical-dynamical approach, whereas Di et al. (2011) and Xie et al. (2012) each developed a quasi two-dimension and quasi three-dimension variably saturated groundwater flow model. These works focused on the temporal and spatial variation of the groundwater table and soil moisture in a riverbank. However, the impacts of river-aquifer water exchange on ecological-hydrological processes, including energy and vapor fluxes, gross primary productivity (GPP) and net ecosystem exchange (NEE) for the riparian ecosystem are not fully represented in previous research. In this study, ~~we incorporated~~ a scheme for stream-aquifer water interaction were

带格式的：缩进：首行缩进： 1 字符

combined with ~~into~~ the Community Land Model Version 4.5 (CLM4.5), which contains descriptions about the energy, biophysical and biochemical processes of the land surface and sub-surface, to investigate the effects of stream-aquifer interaction over 5 cross-sections in the middle reaches of Heihe River Basin, a typical region having an arid climate. Overall, the objectives ~~aims~~ of the study is: (1) ~~Developing the Incorporating a scheme of stream-aquifer water interaction to land surface model CLM4.5 to make it proper to reproduce the process of riverbank hydrology~~ Combining the scheme of stream-aquifer interaction and the land model CLM4.5; (2) Quantifying the magnitudes of ~~the magnitudes of~~ the responses of the riparian hydrological and ecological processes to the stream-aquifer water interaction; (3) Quantifying the maximum ~~propagation~~ distance that the stream –water lateral flow ~~conveyance~~ can affect along the riverbank, and studying the relationship between the magnitude of the effects and the distance to river.–

In Sect. 2 of this paper, the model description about the stream-aquifer interaction scheme and CLM4.5 ~~model development~~ are specifically described, while some background information about the study domain and the experimental design are described in Sect. 3. Section 4 contains the results of simulations and the corresponding analysis. The conclusions and discussion are presented in Sect. 5.

2 Model Description~~development~~

2.1 Community Land Model4.5

The land surface model CLM4.5 was developed by the National Center for Atmospheric Research (Oleson et al., 2013), and is the land component of the Community Earth System Model 1.2.0 (Gent et al., 2011; Hurrell et al., 2013). The CLM4.5 model simulates the biogeophysical exchange of radiation, sensible and latent heat flux; momentum between the land and atmosphere as modified by vegetation and soil; heat transfer in soil and snow; and the hydrologic cycle including precipitation interception, infiltration, runoff, soil water, groundwater table depth and snow dynamics (Lindsay et al., 2014). Bio-geochemical cycles including processes of the carbon and nitrogen cycles, photosynthesis, vegetation phenology, decomposition, and fire disturbances are also presented in CLM4.5. Evapotranspiration simulated by CLM4.5 is partitioned into evaporation and transpiration regulated by stoma physiology and photosynthesis. Specifically, in the CLM4.5 a non-linear groundwater reservoir model is used, but it ~~CLM4.5~~ is basically a one-dimensional model ~~in which physical and chemical processes are considered only in the vertical direction (lateral transits of water and energy are not included yet~~

which only explicitly accounts the ~~effects of~~ vertical recharge from soil layer to aquifer on the dynamics of groundwater table~~)~~. Though a subsurface runoff scheme is applied, it does not explicitly solve the lateral flow and is only suitable in the large-scale modeling. More information about CLM4.5 is contained in the Journal of Climate (http://journals.ametsoc.org /page/CCSM4/CESM1).

2.2 Configuration of CLM4.5 for simulation over riverbank

Generally CLM4.5 is used for large-scale simulations (global/continental) using relatively coarse grid resolution (about 0.1-1 degree), and these simulations usually make use of a horizontal-2D grid structure. However, in the investigation of the effects of stream-aquifer water interaction over riverbank (~~,~~ especially the intensities of these effects with different distances to river), only the one-dimensional~~1D~~ direction perpendicular to the river is matter. Furthermore, the spatial scale of the stream-aquifer interaction is usually restricted within several hundred meters. So some ~~to make the CLM4.5 suitable in the 1D and fine-scale simulation, some modifications and~~ special modifications and configurations ~~settings~~ should be conducted~~done for CLM4.5~~ to make the model suitable for t~~in t~~he one-dimensional~~1D~~ and fine-scale simulation.

As an example, t~~T~~o a certain ~~riverbank on one side of a~~ cross-section~~the stream river, achieve these,~~ we first made the one-dimensional ~~(1×50 in this study))~~ surface dataset ~~—~~used in CLM4.5 simulation for the ~~one-side~~ riverbank using surfacedata-generated tool (Kluzek 2012~~Reference)~~). The ~~–~~schematic diagram for these one-dimensional~~1D~~ grids of the surface dataset was shown in Figure 1c ~~(m=50).~~ A~~A~~at this time, the longitude and latitude values of each grid were~~as~~ set ~~chosen~~ arbitrarily because they would be ~~were~~ modified later)~~the.~~ ~~and~~ Tthen we changed the longitude and latitude of each grid to make them~~it~~ represent ~~corresponding to~~ the real location of each site over the riverbank. Next, we replaced each grid's the elevation, terrain slope, maximum fractional saturated area, land cover types (bare ground~~,~~ ~~vegetation~~vegetation, lakes, etc.~~, etc.~~) and soil types (percentage of clay, silt, ~~and~~ sand and soil organic matter) ~~of the surface dataset~~ of ~~over each grid of~~ the surface dataset with high-resolution ~~dataset of~~ ASTER Dem Dataset (Hirano ~~Akira~~ et al. 2003; Li et al. 2011), MICLCover (Ran et al. 2012), HiWATER Land Cover M~~m~~ap ~~and HJ-CCD Iimage Ddataset (LiZhongLiao~~ et al. 2013~~43~~), and China Soil Characteristics Dataset (Shangguan et al. 2012) ~~according to the real~~. At last, the subsurface runoff scheme in CLM4.5 ~~(as estimated using a non-linear reservoir model)~~ was turned off because it was not suitable in the fine-scale modeling and would be replaced by the groundwater lateral flow in stream-aquifer interaction scheme (described in the Sect.

带格式的：字体：加粗

带格式的：缩进：首行缩进： 1 字符

带格式的：字体颜色：自动设置

带格式的：字体颜色：自动设置

带格式的：字体颜色：自动设置

带格式的：字体颜色：红色

带格式的：字体颜色：自动设置

带格式的：字体颜色：红色

带格式的：字体颜色：自动设置

带格式的：字体颜色：自动设置

带格式的：字体颜色：自动设置

2.3, which was the explicit representation of the subsurface process) ~~subsurface runoff process~~. All the vertical biogeophysical and biogeochemical processes of CLM4.5 was retained because they were~~are~~ not scale-dependent and could ~~an~~ be used in any resolution if the corresponding~~ing~~ surface dataset was set properly.~~we Then we modified the code of CLM4.5 so that all the calculation using the latitude and longitude of grid (most of them are related to radiation) applied the location information of the stream. each . And then~~

带格式的：字体：（中文）+中文正文（宋体），字体颜色：红色

2.3~~2~~ Scheme for stream-aquifer interaction and its implementation into CLM4.5~~Scheme for stream-aquifer interaction and its implementation into CLM4.5~~

The stream-aquifer water interaction scheme (including groundwater lateral flow) developed by Di et al. (2011) was combined with ~~incorporated into~~ CLM4.5 (the combined model was~~and~~ called CLM_RIV). We first describe the new model briefly as follows. Based on Darcy's law and the Dupuit approximation (Bear, 1972), the lateral flow between a river and the neighboring groundwater can be expressed as:

$$R(x,t)=\frac{\partial Q}{\partial x}=\frac{\partial}{\partial x}\left(T(x,t)\frac{\partial h(x,t)}{\partial x}\right), x>0, t\geq 0, \quad (1)$$

while the corresponding initial and boundary conditions are expressed as:

$$h(x,0)=h_0(x), \quad (2)$$

$$h(0,t)=h_{river}(t), \quad (3)$$

where x (L) is the perpendicular distance from the point on a bank to the river channel, t (T) is time, $R(x,t)$ (L/T) is the lateral groundwater recharge (or discharge) rate at point x and time t, Q [L^2/T] is the lateral flow discharge, $T(x,t)$ (L^2/T) is the lateral flow transmissivity, $h(x,t)$ (L) is the groundwater table elevation, $h_0(x)$ (L) is the initial groundwater table elevation and $h_{river}(t)$ (L) is the river water level, as shown in Figures 1a and 1b. If the river water level is higher in elevation than its neighboring groundwater table (as shown in Figure 1a), $R(x,t)$ is greater than zero and the local aquifer is recharged by the stream; otherwise, as shown in Figure 1b, $R(x,t)$ is less than zero and the local aquifer discharges to the stream.

To combine ~~incorporate~~ the stream-aquifer interaction scheme with ~~into~~ CLM4.5, the continuity Eq. (1) should be

discretized over ~~a model~~the one-dimensional~~1D~~ grids of the surface dataset of CLM4.5 (Figure 1c) ~~grid and each variable should be linked to CLM4.5~~. Applying the zero-flux boundary condition to the outermost grid of the simulation domain, the discrete formation of Eq. (1) can be written as:

$$\begin{cases} R_{1,n} = \dfrac{\dfrac{T_{0,n}+T_{1,n}}{2}\times\dfrac{h_{rn}-h_{1,n}}{\Delta x/2}}{\Delta x} - \dfrac{\dfrac{T_{1,n}+T_{2,n}}{2}\times\dfrac{h_{1,n}-h_{2,n}}{\Delta x}}{\Delta x} \\ R_{i,n} = \dfrac{\dfrac{T_{i-1,n}+T_{i,n}}{2}\times\dfrac{h_{i-1,n}-h_{i,n}}{\Delta x}}{\Delta x} - \dfrac{\dfrac{T_{i,n}+T_{i+1,n}}{2}\times\dfrac{h_{i,n}-h_{i+1,n}}{\Delta x}}{\Delta x}, 2 \le i \le m-1, \\ R_{m,n} = \dfrac{\dfrac{T_{m-1,n}+T_{m,n}}{2}\times\dfrac{h_{m-1,n}-h_{m,n}}{\Delta x}}{\Delta x} \end{cases} \quad (4)$$

where i is the number of the grid that is successively added with the increasing distance from grid to channel (Figure 1c), m is the farthest grid from the river channel in the model (i.e., the outermost grid of the simulation domain), n is the number of the time step, $R_{i,n}$ (L/T) is the lateral groundwater recharge (or discharge) rate of grid i at the nth time step, $T_{i,n}$ (L^2/T) is the lateral flow transmissivity, $h_{i,n}$ (L) is the groundwater table elevation, h_{rn} (L)is the river water level (which is another boundary condition of the simulation and will be discussed in Sect. 3.2), and Δx (L) is the side length of each model grid.

The variables $h_{i,n}$, $T_{i,n}$ and $R_{i,n}$ ($i > 0$) in Eq. (4) are linked to CLM4.5 as follows. The water table elevation $h_{i,n}$ is easily obtained by subtracting the groundwater table depth from the ground elevation as:

$$h = h_e - z_{wt}, \quad (5)$$

where h_e (L) and z_{wt} (L) are, respectively, the ground elevation and current groundwater table depth of the grid calculated by CLM4.5. To obtain the lateral flow transmissivity $T_{i,n}$, we considered two cases in the model. In case A, the groundwater table is within the soil layers of the model (i.e., water table lies within 3.8m from surface ~~water table depth is deeper than 3.8m~~) and the transmissivity can be expressed as:

$$T = T_1 + T_2, \quad (6)$$

$$T_1 = \begin{cases} K_i \times \left(z_{h,i} - z_{wt} \right) + \sum_{j=i+1}^{10} K_j \Delta z_j, i < 10 \\ K_{10} \times \left(z_{h,10} - z_{wt} \right), i = 10 \end{cases}, \quad (7)$$

$$T_2 = \int_0^\infty K(z') \, \mathrm{d}z' = \int_0^\infty K_{10} e^{-\frac{z'}{f}} \, \mathrm{d}z' = K_{10} f, \quad (8)$$

where T_1 (L^2/T) and T_2 (L^2/T) are respectively~~is~~ the lateral flow transmissivity within and outside~~in~~ the 10th soil layers of CLM4.5, ~~T_2 (L^2/T) is the transmissivity out of the 10th soil layers,~~ j is the number of soil layer denoted by CLM4.5, K_j (L/T) and f (L) are, respectively, the lateral hydraulic conductivity of the j^{th} soil layer and the e-folding length (which will be discussed later), ~~and~~ Δz_j (L) is the thickness of the j^{th} soil layer, i is the soil layer where ~~within which~~ the groundwater table lies ~~in~~, $z_{h,i}$ (L) is the lower boundary depth ~~bottom level~~ of the i^{th} soil layer ~~i (in depth)~~, z' (L) is the relative depth to the bottom boundary of the 10th~~th~~ soil layer (where $z' = z - 3.8$, $z > 3.8$ m), and $K(z')$ (L/T) is the lateral hydraulic conductivity at relative depth z'.~~.~~ Based on Fan et al. (2007), we also applied an estimation of the lateral hydraulic conductivity at depth below the 10th soil layer in Eq. (8) as:

$$K(z') = K_{10} e^{-\frac{z'}{f}}, \quad (9)$$

~~where K_{10} (L/T) is the lateral hydraulic conductivity at the 10th soil layer, z' (L) is the relative depth to the bottom boundary of the 10th soil layer, and $K(z')$ (L/T) is the lateral hydraulic conductivity at relative depth z'.~~ In CLM4.5, only the vertical hydraulic conductivity is provided. So to obtain the lateral hydraulic conductivity K_j of each soil layer, we applied the assumption of Fan et al. (2007) such that the lateral conductivity is related to the vertical hydraulic conductivity and the content of clay for local soil as:

$$K_j = K_j' \times P_{clay}, \quad (10)$$

where K_j' (L/T) is the vertical hydraulic conductivity provided by CLM4.5 and P_{clay} is the percentage of clay in local soil, as provided by surface data of CLM4.5. The e-folding length f in Eq. (8) is a parameter representing the local

带格式的：上标
带格式的：上标
带格式的：上标
带格式的：字体：倾斜
带格式的：字体：非倾斜
带格式的：上标
带格式的：字体：倾斜
带格式的：字体：倾斜
带格式的：上标
带格式的：缩进：首行缩进： 1 字符

sediment-bedrock profile, which is complex depending on tectonics, weathering and erosion-deposition processes. In this study, we simply implemented an estimation of Fan et al. (2007) to relate e-folding length to terrain slope as:

$$f = \begin{cases} \dfrac{20}{1+125\beta}, \beta \le 0.16 \\ 1, \beta > 0.16 \end{cases}, \quad (11)$$

where ß(radian) represents the terrain slope and can be obtained from the surface data of CLM4.5.

In case B, where the groundwater table is positioned below the 10th soil layer of CLM4.5, the $T_{i,n}$ can be calculated as:

$$T = \int_{z_{wt}-3.8}^{\infty} K(z')\mathrm{d}z' = \int_{z_{wt}-3.8}^{\infty} K_{10} e^{-\frac{z'}{f}} \mathrm{d}z' = K_{10} f e^{\frac{3.8-z_{wt}}{f}}, \quad (12)$$

~~where z_{i10} (L) is the lower boundary depth of the 10th soil layer of CLM4.5.~~ We also applied the parameterization of Eq. (9) in Eq. (12).

In Eq. (4), $T_{0,n}$ (L^2/T) is the flow transmissivity of the river with respect to groundwater-river exchange. Based on Xie and Yuan (2010), flow transmissivity can be expressed as:

$$T_0 = K_r w, \quad (13)$$

where w (L) is the river width obtained from measured data and K_r (L^2/T) is the hydraulic conductivity at the river bed (which will be discussed in Sect. 3.2). —

~~**2.32 Combining the stream-aquifer water interaction scheme with CLM4.5**~~

~~Generally CLM4.5 is used for large-scale simulations (global/continental) using relatively coarse grid resolution (about 0.1-1 degree), and these simulations usually make use of a horizontal 2D 2D lateral grid structure. However, in the investigation of the effects of stream-aquifer water interaction over riverbank over riverbank, (especially the intensities of these effects at sites with different distances to river), only the 1D direction which is perpendicular to the river is matter. Furthermore, the spatial scale of for the stream-aquifer interaction is usually restricted within several hundreds meters. So to make the CLM4.5 suitable in the 1D and finetiny-scale simulation, some modifications and special settings should be~~

带格式的：定义网格后不调整右缩进，无孤行控制，不调整西文与中文之间的空格，不调整中文和数字之间的空格

带格式的：字体：（中文）宋体，加粗

带格式的：缩进：首行缩进： 0 字符

done for CLM4.5, forof CLM4.5 for the CLM4.5 should be done in first to make it suitable for the 1D and tiny-scale simulation. . So we So

Finally, Finally, tTthe lateral water recharge (or discharge) rate $R_{i,n}$ in Eq. (4) is linked to CLM4.5 as follows:

$$\begin{cases} z_{wt\_new} = z_{wt\_ori} - \dfrac{R \times \Delta t}{s_y} \\ W_{new} = W_{ori} + R \times \Delta t \end{cases}, \quad (14)$$

where Δt (T) is the time step of CLM4.5, s_y is the aquifer specific yield calculated by CLM4.5, z_{wt_ori} (L) and z_{wt_new} (L) are, respectively, the original simulated groundwater table depth by CLM4.5 and the updated value after considering the later flow flux, and W_{ori} (L) and W_{new} (L) are, respectively, the original simulated aquifer water storage by CLM4.5 and the updated value after considering the lateral flow flux.

Equations (4) to (14) are applied incorporated in CLM4.5 to renew the values of groundwater table depth and aquifer water storage at every time step. Other hydrological and ecological variables will be in turn be modified by these changes as the model continues to operate. Additionally, the subsurface runoff calculation in the original version of CLM4.5 was turned off and replaced by our lateral flow scheme because in fact groundwater lateral flow was an explicit representation for the subsurface runoff process in the model.

Besides the hydrological and ecological processes, the thermal processesemperature of soil and ground are also affected by the stream-aquifer water interaction. In CLM4.5, the ground and soil heat transfer algorithm is applied on the vertical direction as:

$$c\frac{\partial T}{\partial t} = \frac{\partial}{\partial z}\left[\lambda \frac{\partial T}{\partial z}\right], \quad (15)$$

where z (L) is in the vertical direction and is positive downward, T (K) is the temperature, c (J L^{-3} K^{-1}) is the volumetric soil heat capacity, λ (W L^{-1} K^{-1}) is the thermal conductivity and t (T) is time. The upper (surface) boundary condition of Eq. (15) is got from radiation calculation of CLM4.5, and the lower boundary condition is set as zero-flux situation. Both the thermal properties of c and λ depend on the soil water content as follow (assuming no soil ice for concise expression):

域代码已更改

$$c = c_s\left(1-\theta_{sat}\right)+c_{liq}\theta_{liq}, \quad (16)$$

$$\lambda = K_e\lambda_{sat}+\left(1-K_e\right)\lambda_{dry}, \quad (17)$$

$$K_e = \lg\left(\frac{\theta_{liq}}{\theta_{sat}}\right)+1, \quad (18)$$

where c_s (J L^{-3} K^{-1}) and c_{liq} (J L^{-3} K^{-1}) are respectively the heat capacity of soil solids and liquid water, θ_{sat} (L~~m~~^{3} /L~~m~~$^{-33}$) and θ_{liq} (L^3 L^{-3})(~~m^3/m^3~~) are respectively the saturated soil moisture and current soil liquid water content, λ_{sat} (W L~~m~~$^{-1}$ K^{-1}) and λ_{dry} (W L~~m~~$^{-1}$ K^{-1}) are respectively the saturated thermal conductivity and dry thermal conductivity, and K_e is the Kersten number. More detailed information about the heat transfer calculation can be found in the Chapter 6 of technical description of CLM4.5 (Oleson et al. 2013). As shown by equations (15)-(18), soil moisture θ_{liq} impacted by stream-aquifer water interaction would indirectly affect the simulated temperature and the other thermodynamic variables. Currently, the river temperature and the horizontal heat transfer are not included, but will be incorporated to our model in the future.

域代码已更改

域代码已更改

域代码已更改

带格式的：缩进：首行缩进： 0 字符，无孤行控制

带格式的：缩进：首行缩进： 0 字符，无孤行控制

3 Study domain and experimental design

3.1 Study domain

The Heihe River Basin is the second largest inland river basin in an arid area in Northern China. It is located between 96°42′E and 102°00′E and between 37°41′N and 42°42′N (Lu et al., 2003) (Figure 2). The basin covers 116,000 km^2 and lies to the east of the Shule River Basin and west of the Shiyan River Basin (Chen et al., 2005). In the upper reaches of the basin with obvious vertical zonal divisions, the mean annual precipitation is approximately 200 mm at elevations from 2000 m to 3200 m, and about 500 mm at elevations between 3200 m and 5500 m. The upper reaches are the main water resource of the entire basin (Wu et al., 2010). In the middle reaches, the elevation decreases from 2000 m to 1000 m and the precipitation correspondingly decreases from 200 mm to less than 100 mm in the direction from south to north (Li et al., 2001). The lower reaches, whose mean altitude is approximately 1000 m, is an arid region with a mean annual precipitation of only 42 mm

according to statistics from meteorological stations (Qi and Luo, 2005).

In this study, five typical river cross-sections were chosen as test sites to simulate using our CLM_RIV model. These sites were named, respectively, 213 Bridge, 312 Bridge, Tielu Bridge, Pingchuan Bridge and Gaotai Bridge, and all are located on the middle reaches of the Heihe River Basin. Among these sites, the 213 Bridge section was chosen to test the model's sensitivity, but all the five cross-sections were used in the actual model runs. The locations of these sections and relevant information about them are shown in Figure 3 and Table 1, respectively~~., and the soil types and vegetation types over both sides of the selected sections are shown in Table 2.~~.

3.2 Experimental design

Some ideal experiments to test the model sensitivity to river water level and river bed water conductivity were established for the 213 Bridge section. The CLM_RIV model was run at this section to simulate a riparian zone within 3000 m of the southeast riverbank using a horizontal resolution of 60 m. The simulation period covered the whole year of 2012 using a time step of 1800 s. The atmospheric forcing data were obtained from the China Meteorological Administration Land Data Assimilation System (CLDAS) and developed by the National Meteorological Information Center (NMIC). This high-quality data set combines field observations, remote sensing data and numerical products at a horizontal resolution of 0.0625 degrees. Initial conditions for the simulation were obtained from a 700-year "spin-up" run conducted using the original version of CLM4.5 (without groundwater lateral flow) and cyclically using the CLDAS dataset. ~~We conducted two sensitivity experiments~~ The choice of 700 "spin-up" years was based on the user's guide of CLM (Chapter 4 of Kluzek 2013) showing that when the biogeochemistry carbon-nitrogen module of CLM is turned on, the model should be at least run for 700 years to get a steady state because the magnitudes of carbon and nitrogen fluxes are very small (Oleson et al. 2013). For each situation~~,~~ ~~case (~~**~~a~~**~~)~~ the river recharging groundwater and case (~~**b**~~) the groundwater recharging river~~,~~ we conducted two sensitivity experiments for each case. The first of these examined the sensitivity of the model predictions to changes in the river water level. Four constant river elevations were considered: in the case (~~**a**~~)~~,~~ the four river elevations were h_r = 1493.1 m, 1492.1 m, 1491.1 m and 1490.1 m, and in the case (~~**b**~~)~~,~~ the four river elevations were h_r = 1483.1 m, 1478.1 m, 1473.1 m and 1468.1 m. The hydraulic conductivity of the river bed (K_r) was fixed at 7.4 m d^{-1} for both cases. The second experiment tested the sensitivity of the model to changes in the hydraulic conductivity of the

带格式的：字体颜色：自动设置

带格式的：字体颜色：自动设置

带格式的：字体：（默认）Times New Roman，10 磅，非加粗

带格式的：字体：加粗

带格式的：字体：加粗

带格式的：字体：加粗

带格式的：字体：加粗

river bed. In this experiment, the boundary condition of the river water level was fixed at h_r = 1491.1 m in the case (**a**) and h_r = 1478.1 m in the case (**b**). The ~~and f~~four sets of river hydraulic conductivities were prescribed: K_r = 3 m d^{-1}, 6 m d^{-1}, 12 m d^{-1} and 24 m d^{-1} both for cases.~~.~~

Then to investigate the eco-hydrological effects of stream-aquifer interaction, a "realistic" simulation and a "control" simulation using CLM_RIV were conducted. The realistic simulation (called TEST) reproduced processes of stream-aquifer interaction and groundwater lateral flow; the control simulation (called CTL) did not take the stream-aquifer interaction into consideration (assuming no water flux between stream and riverbank as boundary condition) but also accounted the groundwater lateral flow over riverbank ~~(assuming no water flux between stream and riverbank).~~ For the river grid cells in the middle of each section, no simulations with CLM4.5 were performed.~~,~~ In the Each simulation covered a period of a whole hydrological year from 1 July 2012 to 30 June 2013 using a time step of 1800 s. The models were run at the five sections to simulate both sides of the river within a distance of 3000 m from the river channel using a horizontal resolution of 60 m. As with the sensitivity tests, atmospheric forcing data were used from CLDAS as developed by NMIC. However, instead of using the default surface ~~land cover~~ dataset of CLM4.5 (Oleson et al., 2013), we replaced the data of elevation, terrain slope maximum and fractional saturated area with ASTER Dem Dataset (30-m resolution, Hirano ~~Akira~~ et al. 2003; Li et al. 2011), land cover data with MICLCover (1-km resolution, Ran et al. 2012) plus HiWATER Land Cover Map~~HJ-CCD Image Dataset~~ (30-m resolution, Li ~~Zhong Liao~~ et al. 2013~~43~~) and soil data with China Soil Characteristics Dataset (1-km resolution, Shangguan et al. 2012). ~~we replaced these with data from the MICLCover land cover map of the Heihe River Basin developed by Ran et al. (2012).~~ The soil types and vegetation types over both sides of the selected sections are shown in Table 2. Other model parameters, such as ~~, such as~~ the parameters related to atmospheric boundary layer, ~~soil~~ hydrology, ~~and~~ thermodynamics and ~~,~~ vegetation (including root length density), were set as the default settings of CLM4.5. Detailed information about these parameters could be found ~~seen~~ in the technical description of CLM4.5 (Oleson et al. 2013). ~~were set as the default settings of CLM4.5 ()~~

In the TEST and CTL simulations using CLM_RIV, the lateral hydraulic conductivity of river bed (K_r) was set to 7.4 m d^{-1} based on research of Xie and Yuan (2010). The boundary conditions of river water levels (h_r) for the five sections were obtained from the data set of the hydrometeorological observation network, which is operated by Heihe Watershed Allied

带格式的：字体：加粗

带格式的：字体：加粗

带格式的：字体颜色：自动设置

带格式的：字体颜色：自动设置

带格式的：字体颜色：自动设置

带格式的：字体颜色：自动设置

Telemetry Experimental Research (HiWATER, Li et al., 2013; Liu et al., 2014~~5~~). The observations covered all time periods of our simulations with a time interval of 1800 s~~0.5 h~~. First, the TEST and CTL were started from the default initial condition of CLM4.5 (seen in Oleson et al. 2013) and run 700 years under each configuration (with and without stream-aquifer water interaction), cyclically using the atmospheric forcing and observed water level data. Then, the TEST and CTL would start their formal runs from 1 July 2012 to 30 June 2013 using the restart files produced by the former 700-year spin-up.

~~Both the TEST and CTL runs began from restart files of the 700-year spin-up conducted for each configuration, cyclically using the atmospheric forcing and observed water level data.~~

4 Results~~Eco-hydrological effects of stream-aquifer water interaction~~

4.1 Validation

First, we validated our model using results from the sensitivity experiments. Both the responses of groundwater table in short-term (~~within~~ 7 days) and ~~in~~ long-term (~~within~~ 160 days) ~~response of groundwater table to river levels h_r and river bed water conductivitiesy K_r~~ simulations were displayed ~~plotted~~. The results ~~In the case ((a) of) (river recharging groundwater), Figure 4a-4d shows the short-term responses of water table to the different river water levels as the first sensitivity test (described in Sect. 3.2), and Figure 4e-4h shows the short-term responses of water tables to the different river bed water conductivities as the second sensitivity test ()~~ from ~~of~~ ~~of the~~ case (**a**) (river recharging groundwater) were plotted ~~displayed~~ in the Figure 4. Figure 4a-4h show the time series of the simulated groundwater table depths for each grid cell in the first sensitivity experiment (h_r was varied and K_r was held as constant)~~through the first 7 days (Figure 4a-4d) and 160 days (Figure 4e-4h)~~. From the figures ~~them, we can see that the~~ groundwater table depth near the river channel is significantly reduced ~~increased deepened reduced~~ (groundwater head table ~~is~~ elevated~~declinedelevated~~) as the river water level increases~~decreasesincreases~~. This is because, as Eq. (1) shows, the higher river water level induces a greater hydraulic gradient, which enhances lateral recharge to the riparian aquifer. This effect is significant in both short-term and long-term simulations, indicating the essential role of river ~~water~~ level in the controlling of riparian ~~ground~~water table. Figure 4i-4p show the time series of the simulated groundwater table depths for each grid cell in the second experiment (h_r was held as constant and K_r was varied). From the figures, ~~over the~~

带格式的：字体：加粗

带格式的：字体：倾斜

带格式的：字体：倾斜

~~short-term simulation (Figure 4i-4l),~~ the effect of K_r is significant over the short-term simulation (Figure 4i-4l): As the K_r ranged from 3 m d^{-1} to 24 m d^{-1}, the time spent by the nearest grid (to ~~the~~ river) to get the equilibrium state is shortened from 2 days to 0.5 days. However, after ~~over the~~ long-term simulation (Figure 4m-4p), the groundwater table depths ~~variations~~ are similar for all values of K_r, indicating that ~~the~~ equilibrium state of ground~~-ground~~water table ~~equilibrium~~ along the river channel is not very sensitive to K_r compared with h_r. This~~at~~ is because, river bed water conductivity K_r only connects the river and the nearest model grid to the river, while the rest of grids (not next to river) are not directly influenced by K_r and more affected by the lateral hydraulic conductivity ~~–K (in Eq. (9)) of~~the– riverbank soil (in Eq. (9))~~l than the river bed water conductivity K_r~~. The results from case (**b**) (groundwater recharging river) were plotted in the Figure 5. The conclusions from Figure 5 are similar as Figure 4: River level is matter over both short-term and long-term simulations in the controlling of riparian water table, while the ~~while~~ river bed water conductivity is more ~~more~~ important in the ~~the~~controlling of ~~the~~ short-term water table variation than the controlling of long-term water table equilibrium. Figure 4 and Figure 5 jointly validated that our model could reasonably reproduce both the processes of river recharging groundwater ~~as well as the opposite process o~~and~~f~~ groundwater recharging river.~~short-term response of water table to the river level than the equilibrium state of water table after a long-term simulation. .~~

~~in~~In the first sensitivity test (described in Sect. 3.2), we varied the river levels while holding river bed water conductivity constant, which showed (Figures 4a–4d) that the groundwater table depth near the river channel is significantly reduced (groundwater table is elevated) as the river water level increases. This is because, as Eq. (1) shows, the higher river water level induces a greater hydraulic gradient, which enhances lateral recharge to the riparian aquifer. The second experiment tested the sensitivity of the model to changes in the river bed hydraulic conductivity while the holding river level constant. As shown in Figures 4e–4h, although the river hydraulic conductivity ranged widely from 3 m d^{-1} to 24 m d^{-1}, the groundwater table depth variations were similar for all values of conductivity. This means that the groundwater table along

~~the river channel is not very sensitive to K_r compared with h_r. These results allow us to choose K_r rather arbitrarily, while values of h_r must be realistic.~~

Next, we tested our results from the realistic simulation (TEST) using observed data. First of all, we used observation data from the eddy covariance (EC) and automatic weather station (AWS) system of the Bajitan Gobi Desert station (Liu et al., 2011; Li et al., 2013), a part of hydrometeorological observation network operated by HiWATER, to validate our simulation. The Bajitan Gobi Desert station is located at 100.3042 °E, 38.9150 °N (displayed in Figure 3) and an elevation of 1562 m. The station is on the northwest riverbank of the first section (213 Bridge) in our simulation at a distance of approximately 2800 m from the channel. The station contains a 10-m flux tower equipped with a series of EC instruments for flux measurements, and meteorological instruments for regular weather measurements as well as soil temperature and moisture. The underlying surface of this site is Gobi Desert soil with scarce grass and there are few human activities nearby, which benefitted our validation because anthropogenic effects are not considered in the simulation. Figure 6~~5~~ shows the daily variations in the observations of surface soil temperature, surface soil moisture, sensible heat flux and latent heat flux at the Bajitan Gobi station against the corresponding simulated values from the CTL and TEST runs. The initial observation times of the EC and AWS system were, respectively, 14 August 2012 and 19 September 2012, and there was a successive period near June 2013 with missing measurements for both sensible and latent heat flux. Figures 6~~5~~a and 6~~5~~b show that our model can correctly adjust ~~precisely reproduce~~ the surface~~soil~~ temperature throughout the year but yields surface soil moisture predictions that have a significant positive bias in spring and winter. Despite this, TEST ~~CLM_RIV~~ can generally capture the peak value of soil moisture induced by rain events. Figure 6~~5~~c shows that our model is credible for sensible heat flux simulation, albeit with underestimation of this parameter in winter. Figure 6~~5~~d shows that TEST~~CLM_RIV~~ also simulates the latent head flux well in the rain season, but gives a negative bias in the arid season. Compared with CTL, simulated results of the sensible and latent heat fluxes from TEST are closer to observations, while the results of surface soil temperature and moisture are not distinguished between CTL and TEST. Overall~~,~~, the TEST simulation demonstrated a reasonable~~good~~ ability of CLM_RIV to reproduce the observations of important parameters, especially in the wet season when the eco-hydrological effects of stream-aquifer water interaction are dominant.

Next, we tested the ability of our model to simulate the groundwater table, which is a key factor in ecological and

hydrological effects. We compared the results from both the TEST and CTL simulations with groundwater head elevation and groundwater table depth data from observation wells distributed over the middle reaches of the Heihe River Basin (Zhou et al., 2013). There were 46 wells within our simulation domain of the five sections. Figure 76a shows the annual values of our simulated groundwater head elevation from both TEST and CTL runs against the observed groundwater heads at the 46 wells. As shown, if the stream-aquifer water transfer is not accounted (as in the CTL run), there is a significant underestimation of water head at nearly all sites. When river-groundwater exchange is considered (as in the TEST simulation), the negative biases are much reduced because the water transfer raises the water table, and the modeled groundwater levels are very close to the observations for most wells. However, there are still a few meters of deviation between TEST simulated levels and observed levels~~, which indicates the need for further development of our model in the future~~. The conclusions above were also shown, more apparently, by the comparison of groundwater table depth in Figure 76b. Figure 76c shows the spatial distribution of groundwater table depth from observation, TEST and CTL over the Gaotai Bridge, along which the most number of wells were deployed. We can also see that the systematic errors of simulated groundwater tables were obviously reduced along the whole riverbank after the stream-aquifer water interaction was accounted, though a few meters of deviation still existed. The deviation ~~quality~~ of these results may come from ~~beare directly influenced by~~ the chosen saturated hydraulic conductivity values, which in this study were chosen a priori and as such not optimized in any kind of manner.

Next, we checked the model's ability to simulate spatial variability by comparing simulated ground temperature from the CTL and TEST runs with high-resolution remote sensing data from the Advanced Spaceborne Thermal Emission and Reflection Radiometer (ASTER) launched by the United States National Aeronautics and Space Administration (Tachikawa et al., 2011). The ASTER data had been post-processed for the Heihe River Basin by Li et al. (2014). Ground temperature measurements at 90-m resolution were available for five satellite transit events during the summer of 2012. We used relative temperature of the nearest grid to the stream to emphasize spatial variability. ~~The soil and ground and soil heat transfer algorithm in CLM is applied on the vertical direction as:~~

$$c\frac{\partial T}{\partial t}=\frac{\partial}{\partial z}\left[\lambda\frac{\partial T}{\partial z}\right], \quad (15)$$

where z (m) is in the vertical direction and is positive downward, T (K) is the temperature, c (J m^{-3} K^{-1}) is the volumetric soil heat soil capacity, λ (W m^{-1} K^{-1}) is the thermal conductivity and t (s) is time. Both the thermal properties of c and λ depend on the soil water content as follow (assuming no soil ice for concise expression):

$$c=c_s\left(1-\theta_{sat}\right)+c_{liq}\theta_{liq}, \quad (16)$$

$$\lambda=K_e\lambda_{sat}+\left(1-K_e\right)\lambda_{dry}, \quad (17)$$

$$K_e=\lg\left(\frac{\theta_{liq}}{\theta_{sat}}\right)+1, \quad (18)$$

where c_s (J m^{-3} K^{-1}) and c_{liq} (J m^{-3} K^{-1}) are respectively the heat capacity of soil solids and liquid water, θ_{sat} (m^3/m^3) and θ_{liq} (m^3/m^3) are respectively the saturated soil moisture and current soil liquid water content, λ_{sat} (W m^{-1} K^{-1}) and λ_{dry} (W m^{-1} K^{-1}) are respectively the saturated thermal conductivity and dry thermal conductivity, and K_e is the Kersten number. More detailed information about the heat transfer calculation can be found in the Chapter 6 of technical description of CLM4.5 (Oleson et al. 2013). As shown by equations (15)-(18), soil moisture θ_{liq} impacted by stream-aquifer water interaction would indirectly affect the simulated temperature.

The northwest (left) riverbank of the 213 Bridge station was chosen for our comparison because human activities could be neglected there. Figure 87 shows that in four of the five events our TEST model successfully simulated the increase in ground temperature as distance from the channel increases, while the CTL could not reproduce this spatial variability. However, in the fourth event, the spatial variability predicted by the TEST simulation is much lower than that indicated by ASTER data. This may be caused by the fact that ASTER data are not processed with a cloud mask, which causes overestimation of the cooling effects of streamflow on a cloudy day (Li et al., 2014).

4.2 Eco-hydrological effects of stream-aquifer water interaction

4.2.1 Intra-annual responses to river water level

First, we examined the inter-annual responses of eco-hydrological characteristics to river water level variations. Figure 98

域代码已更改

带格式的：字体：倾斜

带格式的：字体：倾斜

带格式的：字体：倾斜

带格式的：字体：倾斜

域代码已更改

域代码已更改

域代码已更改

带格式的：字体：倾斜

shows the intra-annual variations (at 1800-s ~~0.5-h~~ intervals) of water heads and water table depth at 30 m, 90 m, 210 m and 450 m from the channel on the left riverbanks of streams at the five stations, as well as the observed river water levels. As ~~shown~~Figure 9~~8~~a-e show, the 30-m water heads are tightly connected with river levels and have slightly lower elevations and change-frequencies. The 90-m water heads also follow the river level fluctuations but with some time lags, and the elevations are much lower than the river levels and more resistant to change. At 210 m and 450 m from the stream, there is no discernable relation between water table heads and river water levels, and the former are very stable within the year. The performances of simulated water table depth in Figure 9~~8~~f-j are similar as the water head elevations. The Figure 9~~8~~~~is~~ means the region that can receive the intra-annual signal of river level changes by stream-aquifer interaction is restricted within a limited distance from the channel, and the response to this signal is stronger closer to the river than farther away. The time correlation coefficients between groundwater tables across the left riverbanks and the river levels of the five sections are plotted in Figure ~~9~~10. Considering the time lags of the signal transduction, we used the maximum value of cross-correlation coefficients with time lags from 0 to 3 months (at 1800-s~~0.5-h~~ intervals). The standard line where the correlation coefficient passes the 95% confidence level of the Student's t test is also plotted in Figure 10~~9~~. As shown in Figure 10~~9~~, the correlation coefficients between the groundwater tables and river levels are more than 0.9 for locations very near to streams, but decrease rapidly as distances from channels increase. The left riverbanks of the 213 Bridge and Pingchuan Bridge stations are least impacted by intra-annual river fluctuations; only at locations within 200 m from streams at these stations do correlation coefficients pass the Student's t test. The most affected riverbank is located at Tielu Bridge station, where intra-annual river level fluctuations influence the water table elevations as far as 450 m from the stream. Nonetheless, the area impacted by intra-annual river water level fluctuations (i.e., a zone within 450 m of a stream) is much smaller than that impacted by stream-aquifer exchange (i.e., a zone extending to 1800 m from a stream, see Section 4.2.2.).

We then examined the responses of other eco-hydrological characteristics to intra-annual river water level changes. To highlight the outcomes, we show the simulation results at two rather contrasting stations, Tielu Bridge and 213 Bridge; these stations demonstrated the longest and shortest propagation distances, respectively, for river level fluctuation (Figure 10~~9~~). We plot the area-averaged data within a 300-m range from both sides of the streams.

Figure 110 shows the time series of selected daily ecological and hydrological variables predicted by TEST and CTL simulations, as well as the river levels and precipitation within the simulation period for the Tielu Bridge section. Figures 110c and 10d show that the effects of stream-aquifer interaction on surface soil water and surface ice, respectively, are dominant in spring, autumn, and winter. As expected, the effects on surface soil ice are especially noticeable in winter, with values predicted by the TEST simulation nearly five times those predicted by CTL. The relative lack of influence of the high river water level of summer (Figure 110a) on soil water seems contradictory, but can be explained by the precipitation variation shown in Figure 110b; in summer, surface soil is wetted most by precipitation and stream water contributes relatively less to this effect, while in other seasons the stream water can significantly affect the surface soil water (and ice) because rain events are sparse. These conclusions can be checked in Figure 110e, which shows that the effects of stream-aquifer interaction are perennially apparent on deep soil water that is much less affected by rainprecipitation. –

Figure 110g shows that ground temperature is cooled by stream water in spring and summer and warmed in winter, though the amplitudes of these changes are slight compared with seasonal temperature variation. The higher specific heat capacity induced by wetter soil makes soil temperatures more resistant to the influence of air temperature change than when the soil is dry.

Intra-annual impacts on GPP and ecosystem respiration (RE) are shown in Figures 110h and 110i, respectively. Generally, GPP and RE are both strengthened by stream-aquifer water interaction all year except in winter, and the increased GPP (approximately 0.03 mg C m^{-2} s^{-1} in the growing season) is higher than RE (approximately 0.02 mg C m^{-2} s^{-1}) most of the time. These differences enhance the NEE by approximately 0.01 mg C m^{-2} s^{-1} in the growing season, which means that riparian plants fix more CO_2 from May to September than at other times of the year (as Figure 110j shows). However, there is a time period from March to April when RE is enhanced by stream water supplement, while GPP is unaffected. This time lag causes the riparian vegetation to act as a strong carbon source in this period (Figure 110j) instead of a sink as at other times of the year.

The incremental leaf area index (LAI) and evapotranspiration by water recharge from the river are shown in Figures 110k and 10l, respectively. The LAI is much increased from April to December relative to other times and the stream water

supplement can even advance the beginning, and delay the ending, of the growing season for 1–2 months (Figure 11~~0~~k). Predictions from the TEST simulation indicate that LAI is zero near September 2012, corresponding to the dry river water condition around this time (Figure 11~~0~~a); this result underlines the high sensitivity of riparian plant growth to the stream-aquifer water interaction. Figure 11~~0~~l shows that evapotranspiration variability within the year is also highly related to the fluctuation in river level, reemphasizing the key functions of environmental flows for an ecological system.

Figure 12~~1~~ shows the time series of selected daily ecological and hydrological variables predicted by TEST and CTL simulations, as well as the river levels and precipitation within the simulation period for the 213 Bridge section. The conclusions based on TEST and CTL simulations for Tielu Bridge are generally applicable to the section at 213 Bridge as shown in Figure 12~~1~~, which means that the intra-annual responses of eco-hydrological elements to river water level changes are similar at a wide range of sections in this arid region. However, due to the propagation distance of river level fluctuation at the 213 Bridge section being much shorter than at Tielu Bridge (Figure 10~~9~~), the strength of these hydrological and ecological responses is significantly weaker at 213 Bridge than at Tielu Bridge. The differences can be observed by comparing Figures 11~~0~~ and 12~~1~~.

4.2.2 Annual averaged effects of stream-aquifer water interaction along riverbanks

After studying the intra-annual responses of the riparian eco-hydrological system to river water fluctuation, we examined the annual averaged effects of stream-aquifer water interaction on riparian eco-hydrological elements along riverbanks.

Figure 13~~2~~ shows the differences of annual water head between predictions from TEST and CTL simulations and the terrain elevations along the five sections. All sections show stronger effects of elevated water tables closer to the stream than farther away. The water exchange from stream to aquifer can increase the water head at the grid nearest to the stream (30 m from the channel) by 13 m to 22 m. Furthermore, all cross-sections show water table elevations increased by more than 8 m even at sites nearly 2 km from channels. When averaged for the area within 1800 m from either side of the river channel, the groundwater tables rose by approximately 10–20 m at the five sections. These results show that the effects of stream-aquifer water interaction on annual averaged groundwater levels can spread very far by groundwater lateral flow. Thus groundwater studies must consider the impacts of water exchange between a riverbank and river, a point also stressed by other researchers (Miguez-Macho et al., 2007; Chen et al., 2010; Di et al., 2011). As shown by~~in~~ Figure 13~~2~~, t~~T~~he

relationship between the curve shape of elevation ~~topography~~ and ~~changed~~ water head ~~table~~ along riverbank ~~(by river water conveyance)~~ can be generally figured out: When the terrain is relatively flat, an apparent curvature of ~~changed~~ water head ~~table along riverbank~~ is occurred, such as the left side of 213 Bridge and Pingchuan Bridge and the right side of Tielu Bridge; when the curvature of terrain is obvious, the curve of ~~changed~~ water head ~~table~~ is relatively flat such as the left side of 312 Bridge and Tielu Bridge and the right side of Pingchuan Bridge. However, the curve shape of water head ~~table along riverbank~~ is determined by multi-factors such as the groundwater recharge, soil type and~~,~~ aquifer thickness. The ~~The t~~Ttopography is only (maybe the most) influential ~~important~~ one of them. This topographic factor also explained why the effects of river water conveyance are not symmetrical over the left and right sides.~~–~~

带格式的: 字体: (默认) Times New Roman, 10 磅

Figure 1~~4~~3 shows the differences of summer and winter soil moisture (both liquid water and ice are included) predicted by TEST and CTL simulations along the five sections. Predictions at two depths (2 cm and 100 cm) are chosen to represent the surface and deep soil layers, respectively. Figures 1~~4~~3a–1~~4~~3e show that in summer, the deep soil moisture is increased by stream water from 0.08 m^3 m^{-3} to 0.16 m^3 m^{-3} at the grid closest to the channel, and that this wetting effect is weaker as the distance from the river increases. Averaged for the region within 1 km from the stream, the deep soil is wetted by river water by approximately 0.05 m^3 m^{-3} (a 30% increase) at the riverbank. However, the surface soil moisture is nearly unaffected by stream-aquifer interaction because in summer, surface soil moisture is dominated by precipitation and stream water contributes little to the soil moisture changes. This conclusion is verified in Figures 1~~4~~3f–1~~4~~3j. In winter when rain events are sparse, the wetting effects of stream-aquifer interaction on surface soil moisture are apparent at all sections, though the magnitudes are small (only approximately 0.02 m^3 m^{-3}, a 10% increase) compared with the wetting effects on deep soil. Wetter soil supplies more water for riparian plant growth and subsistence than dry soil, especially in the growing season in an arid region, which stresses the necessity of stream-aquifer water interaction in supporting the riparian environment.

The annual averaged ecological effects of stream-aquifer water interaction were also evaluated. Figure 1~~5~~4 shows differences in predicted GPP, RE (both autotrophic and heterotrophic respiration are included) and NEE resulting from TEST and CTL simulations for the summer period. Because there is no vegetation on the northwest (right) side of the 213 Bridge station, all the values are zero (Figure 1~~5~~4a). Figure 1~~5~~4 shows that GPP and RE increased as the distance to the

channel decreased, while NEE increased (with the ecosystem tending to be a carbon sink) by 0.002–0.005 mg C m^{-2} s^{-1} (100–300%). The impacts are evident within a range of approximately 1 km. The strongest effects appeared at Tielu Bridge station with increases of more than 0.05 mg C m^{-2} s^{-1} for GPP and 0.04 mg C m^{-2} s^{-1} for RE, and a decrease of about 0.01 mg C m^{-2} s^{-1} for NEE at the grid nearest to the stream. The influences of stream-aquifer interaction on GPP are stronger than they are on RE at all sections; this difference explains why the stream effects on NEE are negative (carbon sink) and means that riparian vegetation can absorb more CO_2 and grow better when it is closer to the river. These results highlight the maintenance function of stream-aquifer water interaction for a riparian ecosystem, especially in an arid region.

The simulated effects of stream-aquifer interaction on LAI and canopy transpiration (canopy evaporation is also included) in the summer period are provided in Figure 1~~6~~5. Differences in LAI and transpiration predicted by the TEST and CTL simulations show similar spatial patterns at all sections; in close proximity to the river, LAI and transpiration are increased by supplemental water from the stream. The impacted areas are also within approximately 1 km from the channel for most riverbanks. Averaged over the affected area, the transpiration is enhanced by 0.2–1.0 mm d^{-1} (about 100–200%) and LAI is increased by 0.2–1 in summer. The strongest affected section is Tielu Bridge where the LAI and canopy transpiration increased by approximately 5.0 mm d^{-1} and 4 mm d^{-1}, respectively, at the closest grid to the stream (Figure 1~~6~~5c); riverbanks of other sections are less impacted. The similar spatial distributions of LAI and transpiration across riverbanks means that in this arid region, transpiration along the river is mainly controlled by LAI, which will benefit from stream water lateral infiltration. This finding again stresses the essential influence of stream-aquifer water interaction in riparian hydrologic and carbon cycles, as well as in maintaining environmental integrity.

Lastly, we show the effects of stream-groundwater exchange on vertical energy and water fluxes along a river. Figure 1~~7~~6 shows the differences in sensible heat (SH) and latent heat (LH) fluxes predicted by the TEST and CTL simulations for summer and winter. Figures 1~~7~~6a–1~~7~~6e show that the effects on SH and LH in summer display opposite trends along the riverbanks: LH becomes stronger closer to the stream while SH becomes weaker. The stronger LH is due to the enhanced evapotranspiration along the river (Figure 1~~6~~5), which also induces weaker SH. However, the SH and LH trends change in winter. Figures 1~~7~~6f–1~~7~~6j show that both SH and LH exhibit small positive changes closer to riverbanks, though the magnitudes are much smaller than they are in summer; this may be induced by the lower river water level in winter (Figure

98). Because SH and LH are key factors influencing the atmosphere above a plant canopy, local weather and climate would also be modified by the effects of stream-aquifer water interaction; this suggests that when studying local climate in areas that include streams, the effects of surface water should not be ignored.

带格式的：缩进：首行缩进： 1 字符

5 Conclusions and Discussion

In this study, we combinedincorporated a scheme of stream-aquifer water interaction with into the land surface model CLM4.5 to investigate the eco-hydrological effects of stream-aquifer water interaction over riverbank. After sensitivity tests for selected parameters demonstrated the reliability of the combinednew model (CLM_RIV), the model was used to make two simulations to detect the effects of stream-aquifer water interaction on ecological and hydrological processes on riparian banks at five different locations. One simulation was "forced" using observed river water levels. The other "control" simulation did not take stream-aquifer water exchange into consideration. Both simulations covered a period from July 2012 to June 2013. Comparisons of simulation outputs and observations from EC and AWS systems, water wells and remote sensing data demonstrated that CLM_RIV shows considerable ability to reproduce the natural conditions along riverbanks.

The main conclusions of this study are as follows. (1) A riparian groundwater table responds to the intra-annual variation in river water level, but the response areas are limited to within 200–450 m from the stream channel. The correlation coefficient between the groundwater table and river level can reach 0.9 at the nearest model grid to the river, but rapidly decreases as the distance from the river increases. Surface soil liquid water in the rain season is less impacted by river level variation than is deep soil water, which follows the river level fluctuation all year. (2) Over a typical riverbank section (Tielu Bridge), averaged GPP and respiration of riparian vegetation within 300 m from the stream increased by approximately 0.03 mg C m^{-2} s^{-1} and 0.02 mg C m^{-2} s^{-1}, respectively, in the growing season due to increased soil water, resulting in enhanced NEE of approximately 0.01 mg C m^{-2} s^{-1}. Evapotranspiration in this zone also increased (by approximately 3 mm d^{-1}). Furthermore, the growing season of riparian vegetation is also extended by 2–3 months due to the sustaining water recharge from the stream, and even a short-term decline in river level can negatively impact LAI near the stream during the growing season. (3) All impacted ecological and hydrological characteristics are restricted to an area

within approximately 1 km from the channel, and the effects become stronger as distance to the river decreases. These conclusions highlight the functions of stream-aquifer water interaction on sustaining and controlling the riparian ecological system, and indicate the potential benefits of water regulation, such as through artificial stream water conveyance, to maintain stream flow.

However, there are assumptions and limitations of this study that should be noted. Besides the intrinsic uncertainties of CLM and atmospheric forcing (Bonan et al., 2011, 2013; Mao et al., 2012; Wang et al., 2013), the parameters reflecting the land and river conditions in our scheme, such as K_j, K_r and f in Eq. (4)–(14), are highly parameterized based on some simple assumptions to facilitate data collection and computation, while the real states of geological structures and sediment-bedrock profiles are so complex that they are almost impossible to describe accurately. However, the sensitivity experiments and comparison of our results with data from multiple sources (Sect. 4.1) prove that these uncertainties do not significantly affect the simulation ability of CLM_RIV. Another restriction on our results is that human activities, such as irrigation that may take place on riverbanks, are not considered in our model. Such activities could cause our results to deviate considerably from the real situation. Arguably, the aim of this study was to emphasize the effects of stream-aquifer water interaction (which is a totally natural process) on riparian eco-hydrological processes. Thus, ignoring anthropogenic disturbances on riverbanks (such as crop cultivation, irrigation and water diversion), which may interfere with the natural influences we simulated, was a reasonable approach in this research.

Some future studies are also needed. To overcome the uncertainties of parameterization, more systematic experiments to test the sensitivity of model parameters should be conducted, and corresponding observations or more sophisticated estimation approaches for key parameters relating to stream-aquifer interaction are needed~~. Applying our model to other typical regions (even at a global scale) having different climatic and hydrological environments is expected~~. Finally a land-river-atmosphere interaction model that can simulate the water and energy exchange between each component is needed for studying the more comprehensive effects of stream water flows.

Acknowledgements This study was supported by the National Natural Science Foundation of China (Grants 91125016~~, and~~ 41575096 and 41305066) and by the Chinese Academy of Sciences Strategic Priority Research Program under Grant

XDA05110102. We would like to thank Xing Yuan, Xiangjun Tian and Yuanyaun Wang for their assistance with this work and helpful discussion.

References

Arnold, J., Muttiah, R. S., Srinivasan, R., and Allen, P.: Regional estimation of base flow and groundwater recharge in the Upper Mississippi river basin, J Hydrol, 227, 21-40, 2000.

Baskaran, S., Ransley, T., Brodie, R., and Baker, P.: Investigating groundwater–river interactions using environmental tracers, Australian Journal of Earth Sciences, 56, 13-19, 2009.

Bear, J.: Dynamics of Fluids in Porous Media, 1972.

Bonan, G. B., Hartman, M. D., Parton, W. J., and Wieder, W. R.: Evaluating litter decomposition in earth system models with long‐term litterbag experiments: an example using the Community Land Model version 4 (CLM4), Global change biology, 19, 957-974, 2013.

Bonan, G. B., Lawrence, P. J., Oleson, K. W., Levis, S., Jung, M., Reichstein, M., Lawrence, D. M., and Swenson, S. C.: Improving canopy processes in the Community Land Model version 4 (CLM4) using global flux fields empirically inferred from FLUXNET data, Journal of Geophysical Research: Biogeosciences (2005–2012), 116, 2011.

Chen, F., and Xie, Z. H.: Effects of interbasin water transfer on regional climate: A case study of the Middle Route of the South-to-North Water Transfer Project in China, J Geophys Res-Atmos, 115, Artn D11112, Doi 10.1029/2009jd012611, 2010.

Chen, F., and Xie, Z. H.: Effects of crop growth and development on regional climate: a case study over East Asian monsoon area, Clim Dynam, 38, 2291-2305, 10.1007/s00382-011-1125-y, 2012.

Chen, Y., Zhang, D. Q., Sun, Y. B., Liu, X. N., Wang, N. Z., and Savenije, H. H. G.: Water demand management: A case study of the Heihe River Basin in China, Phys Chem Earth, 30, 408-419.

Chen, Y. N., Chen, Y. P., Xu, C. C., Ye, Z. X., Li, Z. Q., Zhu, C. G., and Ma, X. D.: Effects of ecological water conveyance on groundwater dynamics and riparian vegetation in the lower reaches of Tarim River, China, Hydrol Process, 24, 170-177, 10.1002/hyp.7429, 2010.

Chen, Y. N., Zhang, X. L., Zhu, X. M., Li, W. H., Zhang, Y. M., Xu, H. L., Zhang, H. F., and Chen, Y. P.: Analysis on the ecological benefits of the stream water conveyance to the dried-up river of the lower reaches of Tarim River, China, Sci China Ser D, 47, 1053-1064, 10.1360/03yd0101, 2004.

带格式的： 缩进：左侧： 0 厘米，悬挂缩进：2 字符，首行缩进： -2 字符，行距：1.5 倍行距

Contreras, S., Jobbagy, E. G., Villagra, P. E., Nosetto, M. D., and Puigdefabregas, J.: Remote sensing estimates of supplementary water consumption by arid ecosystems of central Argentina, J Hydrol, 397, 10-22, 10.1016/j.jhydrol.2010.11.014, 2011.

Di, Z. H., Xie, Z. H., Yuan, X., Tian, X. J., Luo, Z. D., and Chen, Y. N.: Prediction of water table depths under soil water-groundwater interaction and stream water conveyance, Sci China Earth Sci, 54, 420-430, DOI 10.1007/s11430-010-4050-8, 2011.

Fan, Y.: Groundwater in the Earth's critical zone: Relevance to large-scale patterns and processes, Water Resour Res, 51, 3052-3069, 10.1002/2015WR017037, 2015.

Fan, Y., and Miguez-Macho, G.: Potential groundwater contribution to Amazon evapotranspiration, Hydrol Earth Syst Sc, 14, 2039-2056, 10.5194/hess-14-2039-2010, 2010.

Fan, Y., and Miguez-Macho, G.: A simple hydrologic framework for simulating wetlands in climate and earth system models, Clim Dynam, 37, 253-278, 10.1007/s00382-010-0829-8, 2011.

Fan, Y., Miguez-Macho, G., Weaver, C. P., Walko, R., and Robock, A.: Incorporating water table dynamics in climate modeling: 1. Water table observations and equilibrium water table simulations, J Geophys Res-Atmos, 112, Artn D10125, 10.1029/2006jd008111, 2007.

Gent, P. R., Danabasoglu, G., Donner, L. J., Holland, M. M., Hunke, E. C., Jayne, S. R., Lawrence, D. M., Neale, R. B., Rasch, P. J., Vertenstein, M., Worley, P. H., Yang, Z. L., and Zhang, M. H.: The Community Climate System Model Version 4, J Climate, 24, 4973-4991, Doi 10.1175/2011jcli4083.1, 2011.

Hirano, A., Welch, R., and Lang, H.: Mapping from ASTER stereo image data: DEM validation and accuracy assessment, ISPRS Journal of Photogrammetry and Remote Sensing, 57, 356-370, 2003.

Hurrell, J. W., Holland, M. M., Gent, P. R., Ghan, S., Kay, J. E., Kushner, P. J., Lamarque, J. F., Large, W. G., Lawrence, D., Lindsay, K., Lipscomb, W. H., Long, M. C., Mahowald, N., Marsh, D. R., Neale, R. B., Rasch, P., Vavrus, S., Vertenstein, M., Bader, D., Collins, W. D., Hack, J. J., Kiehl, J., and Marshall, S.: The Community Earth System Model A Framework for Collaborative Research, B Am Meteorol Soc, 94, 1339-1360, Doi 10.1175/Bams-D-12-00121.1, 2013.

Jobbagy, E. G., Nosetto, M. D., Villagra, P. E., and Jackson, R. B.: Water subsidies from mountains to deserts: their role in sustaining groundwater-fed oases in a sandy landscape, Ecol Appl, 21, 678-694, Doi 10.1890/09-1427.1, 2011.

Kluzek, E.: CESM research tools: CLM4 in CESM1. 0.4 user's guide documentation, National Centers for Atmospheric Research, Boulder, 2012.

Li, H., Sun, D., Yu, Y., Wang, H., Liu, Y., Liu, Q., Du, Y., Wang, H., and Cao, B.: Evaluation of the VIIRS and MODIS LST products in an arid area of Northwest China, Remote Sensing of Environment, 142, 111-121, 2014.

Li, X., Cheng, G. D., Liu, S. M., Xiao, Q., Ma, M. G., Jin, R., Che, T., Liu, Q. H., Wang, W. Z., Qi, Y., Wen, J. G., Li, H. Y., Zhu, G. F., Guo, J. W., Ran, Y. H., Wang, S. G., Zhu, Z. L., Zhou, J., Hu, X. L., and Xu, Z. W.: Heihe Watershed Allied Telemetry Experimental Research (HiWATER): Scientific Objectives and Experimental Design, B Am Meteorol Soc, 94, 1145-1160, 10.1175/Bams-D-12-00154.1, 2013.

Li, X., Lu, L., Cheng, G. D., and Xiao, H. L.: Quantifying landscape structure of the Heihe River Basin, north-west China using FRAGSTATS, J Arid Environ, 48, 521-535, DOI 10.1006/jare.2000.0715, 2001.

Li, X., Nan, Z., Cheng, G., Ding, Y., Wu, L., Wang, L., Wang, J., Ran, Y., Li, H., and Pan, X.: Toward an improved data stewardship and service for environmental and ecological science data in West China, Int J Digit Earth, 4, 347-359, 2011.

Liang, X., and Xie, Z. H.: Important factors in land-atmosphere interactions: surface runoff generations and interactions between surface and groundwater, Global Planet Change, 38, 101-114, 10.1016/S0921-8181(03)00012-2, 2003.

Liang, X., Xie, Z. H., and Huang, M. Y.: A new parameterization for surface and groundwater interactions and its impact on water budgets with the variable infiltration capacity (VIC) land surface model, J Geophys Res-Atmos, 108, Artn 8613, 10.1029/2002jd003090, 2003.

Lindsay, K., Bonan, G. B., Doney, S. C., Hoffman, F. M., Lawrence, D. M., Long, M. C., Mahowald, N. M., Moore, J. K., Randerson, J. T., and Thornton, P. E.: Preindustrial-Control and Twentieth-Century Carbon Cycle Experiments with the Earth System Model CESM1(BGC), J Climate, 27, 8981-9005, Doi 10.1175/Jcli-D-12-00565.1, 2014.

Liu, J., Chen, R., Song, Y., Yang, Y., Qing, W., Han, C., and Liu, Z.: Observations of precipitation type using a time-lapse camera in a mountainous region and calculation of the rain/snow proportion based on the critical air temperature, Environ Earth Sci, 73, 1545-1554, 10.1007/s12665-014-3506-0, 2014.

Lu, L., Li, X., and Cheng, G. D.: Landscape evolution in the middle Heihe River Basin of north-west China during the last decade, J Arid Environ, 53, 395-408, 10.1006/jare.2002.1032, 2003.

Mao, J., Thornton, P. E., Shi, X., Zhao, M., and Post, W. M.: Remote Sensing Evaluation of CLM4 GPP for the Period 2000-09*, J Climate, 25, 5327-5342, 2012.

Maxwell, R. M., Chow, F. K., and Kollet, S. J.: The groundwater-land-surface-atmosphere connection: Soil moisture effects on the atmospheric boundary layer in fully-coupled simulations, Adv Water Resour, 30, 2447-2466, 10.1016/j.advwatres.2007.05.018, 2007.

Maxwell, R. M., and Kollet, S. J.: Interdependence of groundwater dynamics and land-energy feedbacks under climate change, Nat Geosci, 1, 665-669, Doi 10.1038/Ngeo315, 2008.

Miguez-Macho, G., Fan, Y., Weaver, C. P., Walko, R., and Robock, A.: Incorporating water table dynamics in climate modeling: 2. Formulation, validation, and soil moisture simulation, J Geophys Res-Atmos, 112, Artn D13108, 10.1029/2006jd008112, 2007.

Milly, P. C., Dunne, K. A., and Vecchia, A. V.: Global pattern of trends in streamflow and water availability in a changing climate, Nature, 438, 347-350, 2005.

Nepstad, D. C., Decarvalho, C. R., Davidson, E. A., Jipp, P. H., Lefebvre, P. A., Negreiros, G. H., Dasilva, E. D., Stone, T. A., Trumbore, S. E., and Vieira, S.: The Role of Deep Roots in the Hydrological and Carbon Cycles of Amazonian Forests and Pastures, Nature, 372, 666-669, Doi 10.1038/372666a0, 1994.

Oleson, K., Lawrence, D., Bonan, G., Drewniak, B., Huang, M., Koven, C., Levis, S., Li, F., Riley, W., and Subin, Z.: Technical Description of version 4.5 of the Community Land Model (CLM), NCAR, National Center for Atmospheric Research (NCAR) Boulder, Colorado, 2013.

Ouyang, Z., Zhao, T., Wang, X., and Miao, H.: Ecosystem services analyses and valuation of China terrestrial surface water system, Acta Ecologica Sinica, 24, 2091-2099, 2003.

Qi, S. Z., and Luo, F.: Water environmental degradation of the Heihe River Basin in arid northwestern China, Environ Monit Assess, 108, 205-215, 10.1007/s10661-005-3912-6, 2005.

Ran, Y., Li, X., Lu, L., and Li, Z.: Large-scale land cover mapping with the integration of multi-source information based on the Dempster–Shafer theory, International Journal of Geographical Information Science, 26, 169-191, 2012.

Scanlon, B. R., Healy, R. W., and Cook, P. G.: Choosing appropriate techniques for quantifying groundwater recharge, Hydrogeol J, 10, 18-39, 2002.

Schär, C., Lüthi, D., Beyerle, U., and Heise, E.: The soil-precipitation feedback: A process study with a regional climate model, J Climate, 12, 722-741, 1999.

Shangguan, W., Dai, Y., Liu, B., Ye, A., and Yuan, H.: A soil particle-size distribution dataset for regional land and climate modelling in China, Geoderma, 171, 85-91, 2012.

Shen, Y., and Chen, Y.: Global perspective on hydrology, water balance, and water resources management in arid basins, Hydrol Process, 24, 129-135, 2010.

Tachikawa, T., Kaku, M., Iwasaki, A., Gesch, D., Oimoen, M., Zhang, Z., Danielson, J., Krieger, T., Curtis, B., and Haase, J.: ASTER Global Digital Elevation Model Version 2–Summary of Validation Results, ASTER GDEM Validation Team (http://www. jspacesystems. or. jp/ersdac/GDEM/ver2Validation/Summary_GDEM2_v alidation_report_final. pdf), 2011.

Tsur, Y., and Graham-Tomasi, T.: The buffer value of groundwater with stochastic surface water supplies, Journal of environmental economics and management, 21, 201-224, 1991.

Wang, K., Mao, J., Dickinson, R. E., Shi, X., Post, W. M., Zhu, Z., and Myneni, R. B.: Evaluation of CLM4 solar radiation partitioning scheme using remote sensing and site level FPAR datasets, Remote Sensing, 5, 2857-2882, 2013.

Wu, J. K., Ding, Y., Ye, B., Yang, Q., Zhang, X., and Wang, J.: Spatio-temporal variation of stable isotopes in precipitation in the Heihe River Basin, Northwestern China, Environ Earth Sci, 61, 1123-1134, 10.1007/s12665-009-0432-7, 2010.

Xie, Z. H., Di, Z. H., Luo, Z. D., and Ma, Q.: A Quasi-Three-Dimensional Variably Saturated Groundwater Flow Model for Climate Modeling, J Hydrometeorol, 13, 27-46, Doi 10.1175/Jhm-D-10-05019.1, 2012.

Xie, Z. H., and Yuan, X.: Prediction of water table under stream-aquifer interactions over an arid region, Hydrol Process, 24, 160-169, Doi 10.1002/Hyp.7434, 2010.

Xie, Z. H., Zeng, N., Wang, H. J., Lin, Z., Tian, X. J., and Jia, B. H.: Past, present and future of the carbon cycle, Natl Sci Rev, 1, 18-21, 10.1093/nsr/nwt021, 2014.

Yu, Y., Xie, Z. H., and Zeng, X. B.: Impacts of modified Richards equation on RegCM4 regional climate modeling over East Asia, J Geophys Res-Atmos, 119, 12642-12659, Doi 10.1002/2014jd021872, 2014.

Zhao, W., and Cheng, G.: Review of several problems on the study of eco-hydrological processes in arid zones, Chinese Sci Bull, 47, 353-360, 2002.

Zou, J., Xie, Z. H., Yu, Y., Zhan, C. S., and Sun, Q.: Climatic responses to anthropogenic groundwater exploitation: a case study of the Haihe River Basin, Northern China, Clim Dynam, 42, 2125-2145, DOI 10.1007/s00382-013-1995-2, 2014.

Zou, J., Xie, Z. H., Zhan, C. S., Qin, P. H., Sun, Q., Jia, B. H., and Xia, J.: Effects of anthropogenic groundwater exploitation on land surface processes: A case study of the Haihe River Basin, northern China, J Hydrol, 524, 625-641, DOI 10.1016/j.jhydrol.2015.03.026, 2015.8

Arnold, J., Muttiah, R. S., Srinivasan, R., and Allen, P.: Regional estimation of base flow and groundwater recharge in the Upper Mississippi river basin, J Hydrol, 227, 21-40, 2000.

Baskaran, S., Ransley, T., Brodie, R., and Baker, P.: Investigating groundwater–river interactions using environmental tracers, Australian Journal of Earth Sciences, 56, 13-19, 2009.

Bear, J.: Dynamics of Fluids in Porous Media, 1972.

Bonan, G. B., Hartman, M. D., Parton, W. J., and Wieder, W. R.: Evaluating litter decomposition in earth system models with long‐term litterbag experiments: an example using the Community Land Model version 4 (CLM4), Global change biology, 19, 957-974, 2013.

Bonan, G. B., Lawrence, P. J., Oleson, K. W., Levis, S., Jung, M., Reichstein, M., Lawrence, D. M., and Swenson, S. C.: Improving canopy processes in the Community Land Model version 4 (CLM4) using global flux fields empirically inferred from FLUXNET data, Journal of Geophysical Research: Biogeosciences (2005–2012), 116, 2011.

Chen, F., and Xie, Z. H.: Effects of interbasin water transfer on regional climate: A case study of the Middle Route of the South-to-North Water Transfer Project in China, J Geophys Res-Atmos, 115, Artn D11112, Doi 10.1029/2009jd012611, 2010.

Chen, F., and Xie, Z. H.: Effects of crop growth and development on regional climate: a case study over East Asian monsoon area, Clim Dynam, 38, 2291-2305, 10.1007/s00382-011-1125-y, 2012.

Chen, Y., Zhang, D. Q., Sun, Y. B., Liu, X. N., Wang, N. Z., and Savenije, H. H. G.: Water demand management: A case study of the Heihe River Basin in China, Phys Chem Earth, 30, 408-419, 10.1016/j.pce.2005.06.019, 2005.

Chen, Y. N., Chen, Y. P., Xu, C. C., Ye, Z. X., Li, Z. Q., Zhu, C. G., and Ma, X. D.: Effects of ecological water conveyance on groundwater dynamics and riparian vegetation in the lower reaches of Tarim River, China, Hydrol Process, 24, 170-177, 10.1002/hyp.7429, 2010.

Chen, Y. N., Zhang, X. L., Zhu, X. M., Li, W. H., Zhang, Y. M., Xu, H. L., Zhang, H. F., and Chen, Y. P.: Analysis on the ecological benefits of the stream water conveyance to the dried-up river of the lower reaches of Tarim River, China, Sci China Ser D, 47, 1053-1064, 10.1360/03yd0101, 2004.

Di, Z. H., Xie, Z. H., Yuan, X., Tian, X. J., Luo, Z. D., and Chen, Y. N.: Prediction of water table depths under soil-water-groundwater interaction and stream water conveyance, Sci China Earth Sci, 54, 420-430, DOI 10.1007/s11430-010-4050-8, 2011.

Fan, Y.: Groundwater in the Earth's critical zone: Relevance to large-scale patterns and processes, Water Resour Res, 51, 3052-3069, 10.1002/2015WR017037, 2015.

Fan, Y., and Miguez-Macho, G.: Potential groundwater contribution to Amazon evapotranspiration, Hydrol Earth Syst Sc, 14, 2039-2056, 10.5194/hess-14-2039-2010, 2010.

Fan, Y., and Miguez-Macho, G.: A simple hydrologic framework for simulating wetlands in climate and earth system models, Clim Dynam, 37, 253-278, 10.1007/s00382-010-0829-8, 2011.

Fan, Y., Miguez-Macho, G., Weaver, C. P., Walko, R., and Robock, A.: Incorporating water table dynamics in climate modeling: 1. Water table observations and equilibrium water table simulations, J Geophys Res-Atmos, 112, Artn D10125, 10.1029/2006jd008111, 2007.

Gent, P. R., Danabasoglu, G., Donner, L. J., Holland, M. M., Hunke, E. C., Jayne, S. R., Lawrence, D. M., Neale, R. B., Rasch, P. J., Vertenstein, M., Worley, P. H., Yang, Z. L., and Zhang, M. H.: The Community Climate System Model Version 4, J Climate, 24, 4973-4991, Doi 10.1175/2011jcli4083.1, 2011.

Hurrell, J. W., Holland, M. M., Gent, P. R., Ghan, S., Kay, J. E., Kushner, P. J., Lamarque, J. F., Large, W. G., Lawrence, D., Lindsay, K., Lipscomb, W. H., Long, M. C., Mahowald, N., Marsh, D. R., Neale, R. B., Rasch, P., Vavrus, S., Vertenstein, M., Bader, D., Collins, W. D., Hack, J. J., Kiehl, J., and Marshall, S.: The Community Earth System Model A Framework for Collaborative Research, B Am Meteorol Soc, 94, 1339-1360, Doi 10.1175/Bams-D-12-00121.1, 2013.

Li, H., Sun, D., Yu, Y., Wang, H., Liu, Y., Liu, Q., Du, Y., Wang, H., and Cao, B.: Evaluation of the VIIRS and MODIS LST products in an arid area of Northwest China, Remote Sensing of Environment, 142, 111-121, 2014.

Li, X., Cheng, G. D., Liu, S. M., Xiao, Q., Ma, M. G., Jin, R., Che, T., Liu, Q. H., Wang, W. Z., Qi, Y., Wen, J. G., Li, H. Y., Zhu, G. F., Guo, J. W., Ran, Y. H., Wang, S. G., Zhu, Z. L., Zhou, J., Hu, X. L., and Xu, Z. W.: Heihe Watershed

Allied Telemetry Experimental Research (HiWATER): Scientific Objectives and Experimental Design, B Am Meteorol Soc, 94, 1145-1160, 10.1175/Bams-D-12-00154.1, 2013.

Li, X., Lu, L., Cheng, G. D., and Xiao, H. L.: Quantifying landscape structure of the Heihe River Basin, north-west China using FRAGSTATS, J Arid Environ, 48, 521-535, DOI 10.1006/jare.2000.0715, 2001.

Liang, X., and Xie, Z. H.: Important factors in land-atmosphere interactions: surface runoff generations and interactions between surface and groundwater, Global Planet Change, 38, 101-114, 10.1016/S0921-8181(03)00012-2, 2003.

Liang, X., Xie, Z. H., and Huang, M. Y.: A new parameterization for surface and groundwater interactions and its impact on water budgets with the variable infiltration capacity (VIC) land surface model, J Geophys Res-Atmos, 108, Artn 8613, 10.1029/2002jd003090, 2003.

Lindsay, K., Bonan, G. B., Doney, S. C., Hoffman, F. M., Lawrence, D. M., Long, M. C., Mahowald, N. M., Moore, J. K., Randerson, J. T., and Thornton, P. E.: Preindustrial-Control and Twentieth-Century Carbon Cycle Experiments with the Earth System Model CESM1(BGC), J Climate, 27, 8981-9005, Doi 10.1175/Jcli-D-12-00565.1, 2014.

Liu, J., Chen, R., Song, Y., Yang, Y., Qing, W., Han, C., and Liu, Z.: Observations of precipitation type using a time-lapse camera in a mountainous region and calculation of the rain/snow proportion based on the critical air temperature, Environ Earth Sci, 73, 1545-1554, 10.1007/s12665-014-3506-0, 2014.

Liu, S., Xu, Z., Wang, W., Jia, Z., Zhu, M., Bai, J., and Wang, J.: A comparison of eddy-covariance and large aperture scintillometer measurements with respect to the energy balance closure problem, Hydrol Earth Syst Sc, 15, 1291-1306, 2011.

Lu, L., Li, X., and Cheng, G. D.: Landscape evolution in the middle Heihe River Basin of north-west China during the last decade, J Arid Environ, 53, 395-408, 10.1006/jare.2002.1032, 2003.

Mao, J., Thornton, P. E., Shi, X., Zhao, M., and Post, W. M.: Remote Sensing Evaluation of CLM4 GPP for the Period 2000-09*, J Climate, 25, 5327-5342, 2012.

Maxwell, R. M., Chow, F. K., and Kollet, S. J.: The groundwater-land-surface-atmosphere connection: Soil moisture effects on the atmospheric boundary layer in fully-coupled simulations, Adv Water Resour, 30, 2447-2466, 10.1016/j.advwatres.2007.05.018, 2007.

Maxwell, R. M., and Kollet, S. J.: Interdependence of groundwater dynamics and land-energy feedbacks under climate change, Nat Geosci, 1, 665-669, Doi 10.1038/Ngeo315, 2008.

Miguez-Macho, G., Fan, Y., Weaver, C. P., Walko, R., and Robock, A.: Incorporating water table dynamics in climate modeling: 2. Formulation, validation, and soil moisture simulation, J Geophys Res-Atmos, 112, Artn D13108, 10.1029/2006jd008112, 2007.

Oleson, K., Lawrence, D., Bonan, G., Drewniak, B., Huang, M., Koven, C., Levis, S., Li, F., Riley, W., and Subin, Z.: Technical Description of version 4.5 of the Community Land Model (CLM), NCAR, National Center for Atmospheric Research (NCAR) Boulder, Colorado, 2013.

Qi, S. Z., and Luo, F.: Water environmental degradation of the Heihe River Basin in arid northwestern China, Environ Monit Assess, 108, 205-215, 10.1007/s10661-005-3912-6, 2005.

Ran, Y., Li, X., Lu, L., and Li, Z.: Large-scale land cover mapping with the integration of multi-source information based on the Dempster–Shafer theory, International Journal of Geographical Information Science, 26, 169-191, 2012.

Scanlon, B. R., Healy, R. W., and Cook, P. G.: Choosing appropriate techniques for quantifying groundwater recharge, Hydrogeol J, 10, 18-39, 2002.

Tachikawa, T., Kaku, M., Iwasaki, A., Gesch, D., Oimoen, M., Zhang, Z., Danielson, J., Krieger, T., Curtis, B., and Haase, J.: ASTER Global Digital Elevation Model Version 2–Summary of Validation Results, ASTER GDEM Validation Team (http://www. jspacesystems. or. jp/ersdac/GDEM/ver2Validation/Summary_GDEM2_v alidation_report_final. pdf), 2011.

Wang, K., Mao, J., Dickinson, R. E., Shi, X., Post, W. M., Zhu, Z., and Myneni, R. B.: Evaluation of CLM4 solar radiation partitioning scheme using remote sensing and site level FPAR datasets, Remote Sensing, 5, 2857-2882, 2013.

Wu, J. K., Ding, Y., Ye, B., Yang, Q., Zhang, X., and Wang, J.: Spatio-temporal variation of stable isotopes in precipitation in the Heihe River Basin, Northwestern China, Environ Earth Sci, 61, 1123-1134, 10.1007/s12665-009-0432-7, 2010.

Xie, Z. H., Di, Z. H., Luo, Z. D., and Ma, Q.: A Quasi-Three-Dimensional Variably Saturated Groundwater Flow Model for Climate Modeling, J Hydrometeorol, 13, 27-46, Doi 10.1175/Jhm-D-10-05019.1, 2012.

Xie, Z. H., and Yuan, X.: Prediction of water table under stream-aquifer interactions over an arid region, Hydrol Process, 24, 160-169, Doi 10.1002/Hyp.7434, 2010.

Xie, Z. H., Zeng, N., Wang, H. J., Lin, Z., Tian, X. J., and Jia, B. H.: Past, present and future of the carbon cycle, Natl Sci Rev, 1, 18-21, 10.1093/nsr/nwt021, 2014.

Yu, Y., Xie, Z. H., and Zeng, X. B.: Impacts of modified Richards equation on RegCM4 regional climate modeling over East Asia, J Geophys Res-Atmos, 119, 12642-12659, Doi 10.1002/2014jd021872, 2014.

Zhao, W., and Cheng, G.: Review of several problems on the study of eco-hydrological processes in arid zones, Chinese Sci Bull, 47, 353-360, 2002.

Zhou, J., Hu, B. X., Cheng, G., Wang, G., and Li, X.: Development of a three‐dimensional watershed modelling system for water cycle in the middle part of the Heihe rivershed, in the west of China, Hydrol Process, 25, 1964-1978, 2011.

Zou, J., Xie, Z. H., Yu, Y., Zhan, C. S., and Sun, Q.: Climatic responses to anthropogenic groundwater exploitation: a case study of the Haihe River Basin, Northern China, Clim Dynam, 42, 2125-2145, DOI 10.1007/s00382-013-1995-2, 2014.

Zou, J., Xie, Z. H., Zhan, C. S., Qin, P. H., Sun, Q., Jia, B. H., and Xia, J.: Effects of anthropogenic groundwater exploitation on land surface processes: A case study of the Haihe River Basin, northern China, J Hydrol, 524, 625-641, DOI 10.1016/j.jhydrol.2015.03.026, 2015.

Table 1 The locations and relevant information about the five selected sections used in simulations.

Number of section	Name	Latitude	Longitude	Width (m)	Riverbank elevation (m)	Bottom elevation (m)	Flow direction
1	213 Bridge	38 °54'43.55"N	100 °20'41.05"E	330	1493.1	1488.8	Northeast
2	312 Bridge	38°59′51.71″N	100°24′38.76″E	70	1402	1397	Northeast
3	Tielu Bridge	39 °2'33.08"N	100 °25'49.42"E	50	1382	1379.25	Northeast
4	Pingchuan Bridge	39 °20'2.03"N	100 °5'49.63"E	130	1323.8	1319	West
5	Gaotai Bridge	39 °23'22.93"N	99 °49'37.29"E	210	1295.5	1288.5	West

Table 2 The soil types and vegetation types over both sides of the five selected sections used in simulations.

Number of section	Name	Soil type (Left)	Soil type (Right)	Vegetation type (Left)	Vegetation type (Right)
1	213 Bridge	Sand	Silt	Bare ground	Corn
2	312 Bridge	Silt	Silt	Corn	Grass
3	Tielu Bridge	Silt	Silt	Corn	Grass and corn
4	Pingchuan Bridge	Silt	Silt	Grass and Corn	Grass and corn
5	Gaotai Bridge	Sand	Sand	Grass	Corn

带格式的：左，行距：单倍行距，孤行控制，不取消行号

带格式的：居中，缩进：左侧： 0 厘米，首行缩进： 0 字符，定义网格后不调整右缩进，行距：2 倍行距，无孤行控制，不调整西文与中文之间的空格，不调整中文和数字之间的空格

带格式的：字体：10 磅

带格式表格

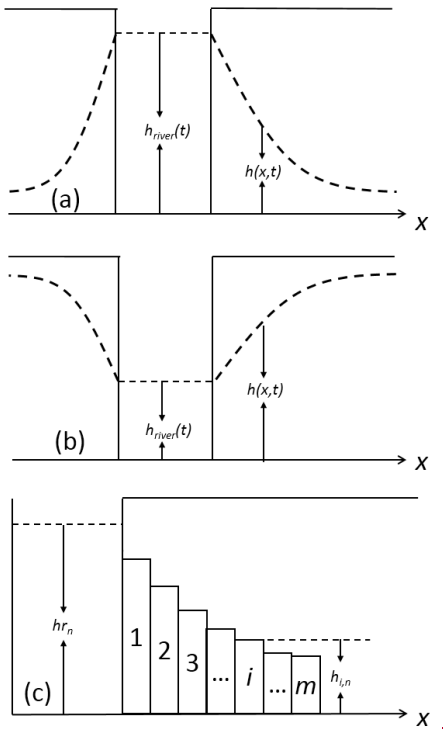
$h_{river}(t)$
$h(x,t)$
(a)
x
$h(x,t)$
$h_{river}(t)$
(b)
x
hr_n
1
2
3
...
i
...
m
$h_{i,n}$
(c)
x

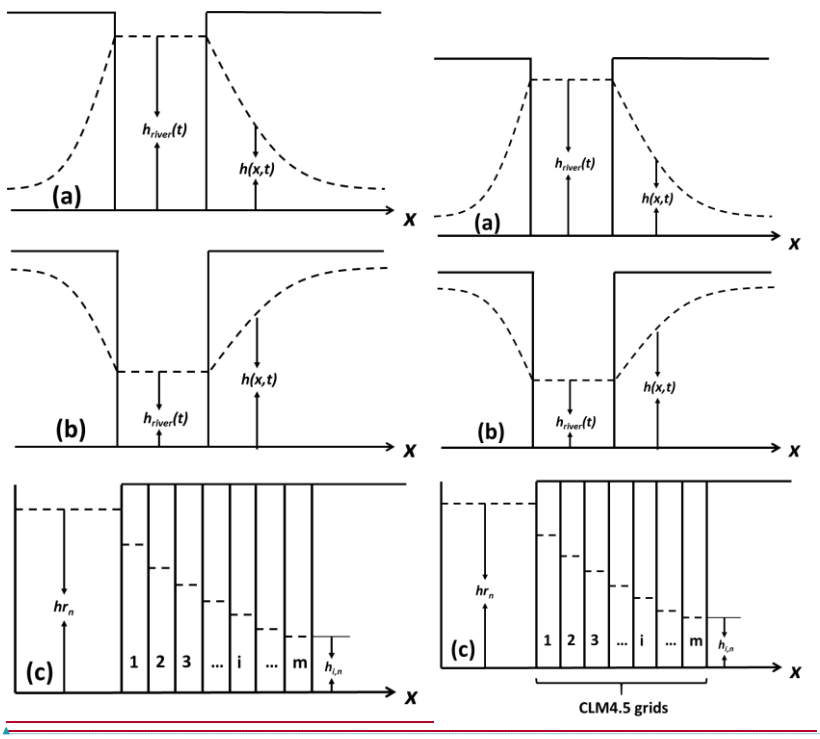

带格式的：字体：（默认）Times New Roman，（中文）Times New Roman，小四

Figure 1 Schematic representation of stream-aquifer water interaction when (a) the river water level is higher than its neighboring groundwater table and (b) the river water level is lower than its neighboring groundwater table. (c) Schematic diagram for horizontal discrete grid cells of a riverbank. The dash lines ~~lengths of the boxes~~ represent the water heads~~, and the widths of the boxes represent the side lengths of the model grids.~~

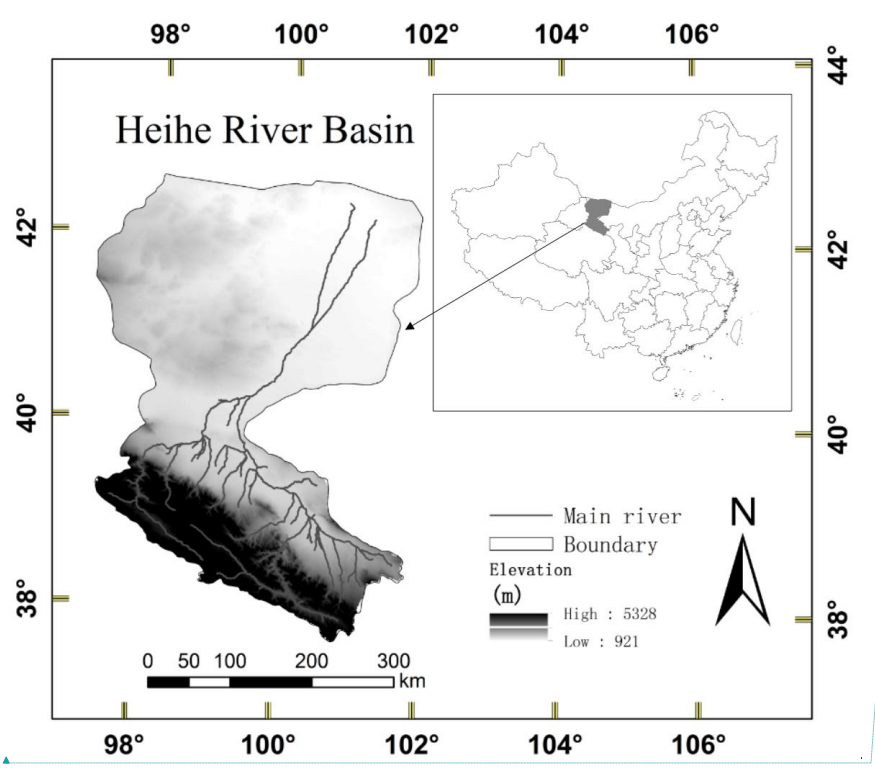
Heihe River Basin
98°
100°
102°
104°
106°
44°
42°
40°
38°
Main river
Boundary
Elevation
(m)
High : 5328
Low : 921
N
0 50 100 200 300
km

带格式的：字体：10 磅

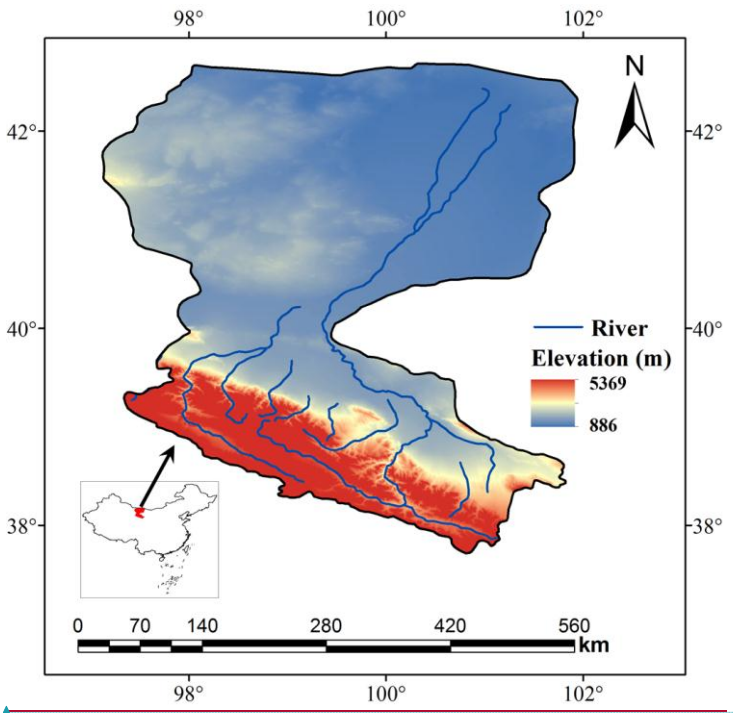

Figure 2 Study area and location of the Heihe River Basin in northwest China.

带格式的: 字体: Times New Roman, 10 磅, 加粗

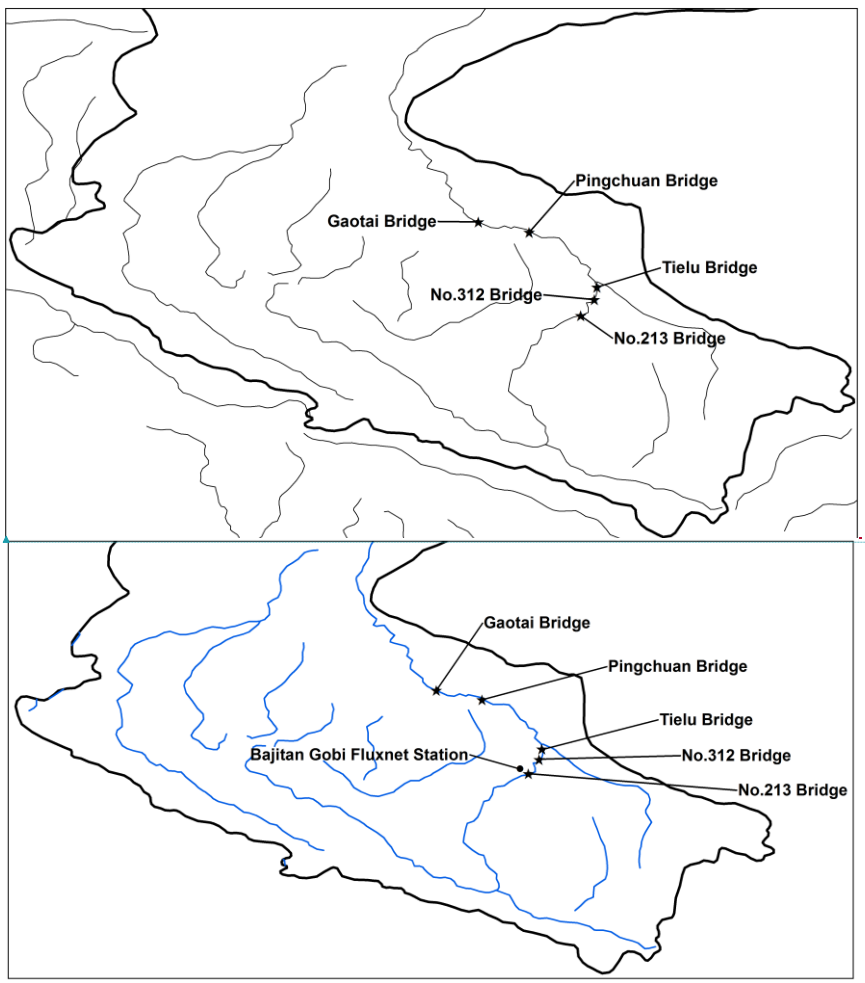

带格式的：字体：(默认) Times New Roman, (中文) Times New Roman, 10 磅

Figure 3 Locations of the five sections in the middle reaches of the Heihe River that were used for

simulations and the location of Bajitan Gobi Fluxnet Station that was used for validation.

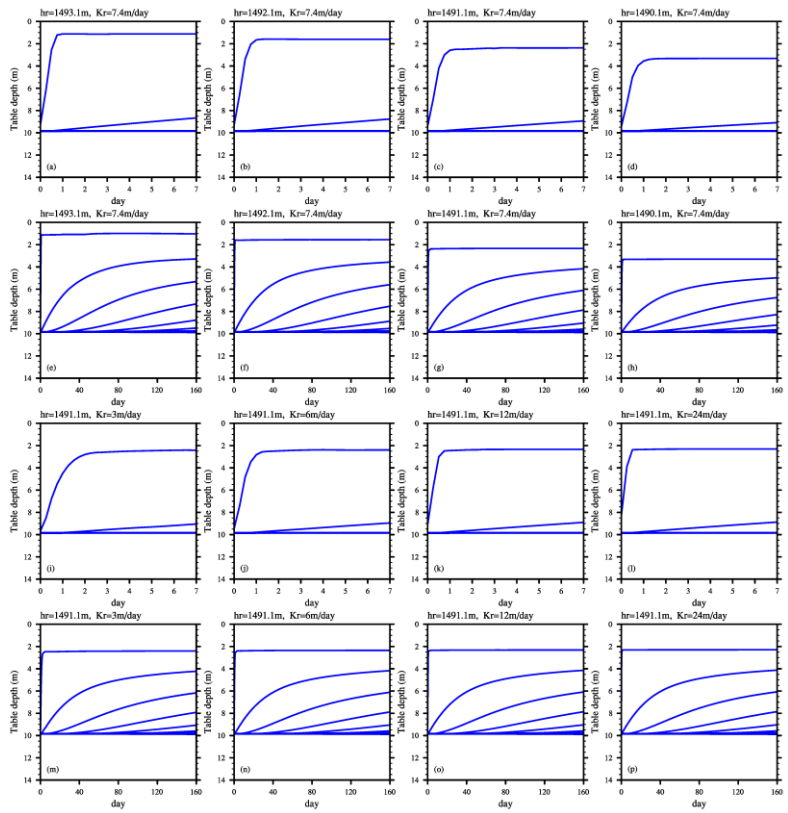

带格式的：字体：Times New Roman，10 磅

带格式的：居中

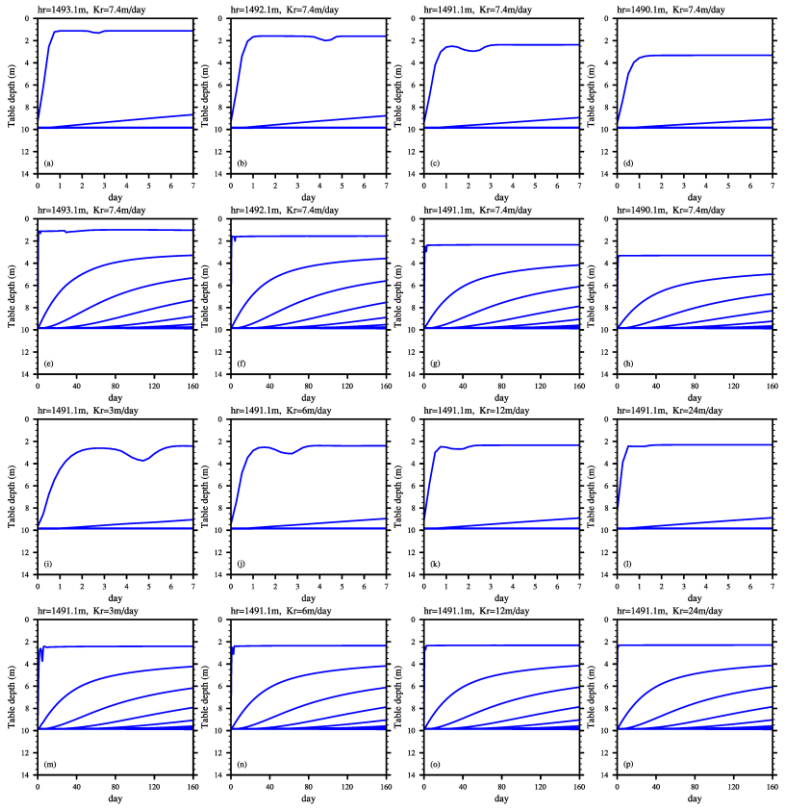
hr=1493.1m, Kr=7.4m/day
hr=1492.1m, Kr=7.4m/day
hr=1491.1m, Kr=7.4m/day
hr=1490.1m, Kr=7.4m/day
hr=1493.1m, Kr=7.4m/day
hr=1492.1m, Kr=7.4m/day
hr=1491.1m, Kr=7.4m/day
hr=1490.1m, Kr=7.4m/day
hr=1491.1m, Kr=3m/day
hr=1491.1m, Kr=6m/day
hr=1491.1m, Kr=12m/day
hr=1491.1m, Kr=24m/day
hr=1491.1m, Kr=3m/day
hr=1491.1m, Kr=6m/day
hr=1491.1m, Kr=12m/day
hr=1491.1m, Kr=24m/day
Table depth (m)
day
(a)
(b)
(c)
(d)
(e)
(f)
(g)
(h)
(i)
(j)
(k)
(l)
(m)
(n)
(o)
(p)

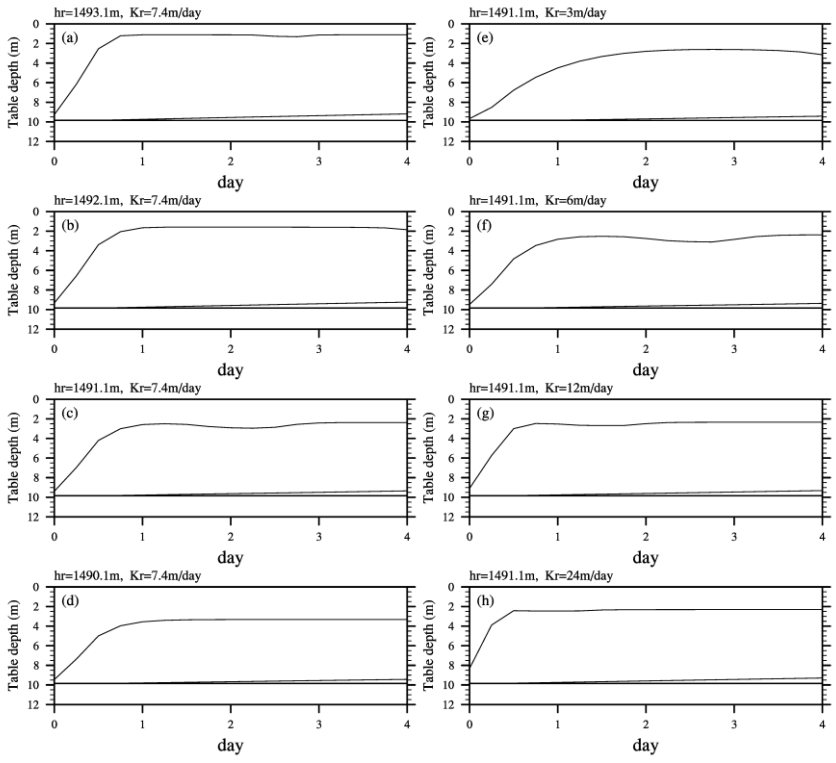
hr=1493.1m, Kr=7.4m/day
(a)
hr=1491.1m, Kr=3m/day
(e)
hr=1492.1m, Kr=7.4m/day
(b)
hr=1491.1m, Kr=6m/day
(f)
hr=1491.1m, Kr=7.4m/day
(c)
hr=1491.1m, Kr=12m/day
(g)
hr=1490.1m, Kr=7.4m/day
(d)
hr=1491.1m, Kr=24m/day
(h)
Table depth (m)
day

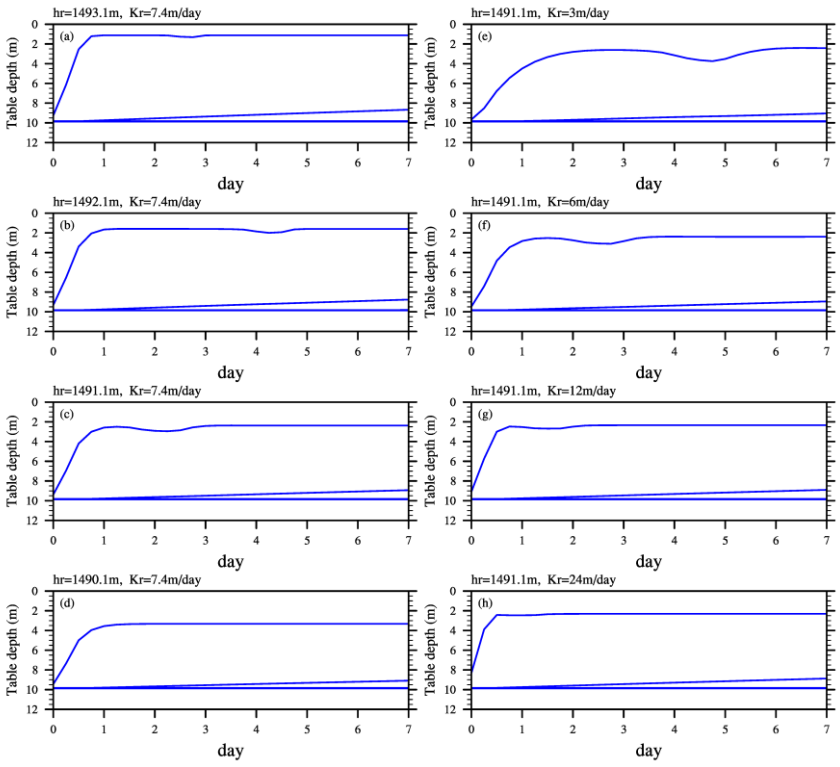

Figure 4 (a-d, i-l) Short-term and (e-h, m-p) long-term ~~Short-term (in 74 days) r~~responses of riparian groundwater table to the river water level h_r and river bed hydraulic conductivity K_r in the case ~~situation~~ of river recharging groundwater. (a-h~~d~~) Time series of the simulated groundwater table depths for each~~20~~ grid cell~~s~~ in the first sensitivity experiment. (i-p~~e~~ ~~h~~) Time series for the second sensitivity experiment.

带格式的： 两端对齐，定义网格后不调整右缩进，行距：2 倍行距，无孤行控制，取消行号，不调整西文与中文之间的空格，不调整中文和数字之间的空格

带格式的： 字体：倾斜

带格式的： 字体：倾斜，下标

带格式的： 字体：倾斜

带格式的： 字体：倾斜，下标

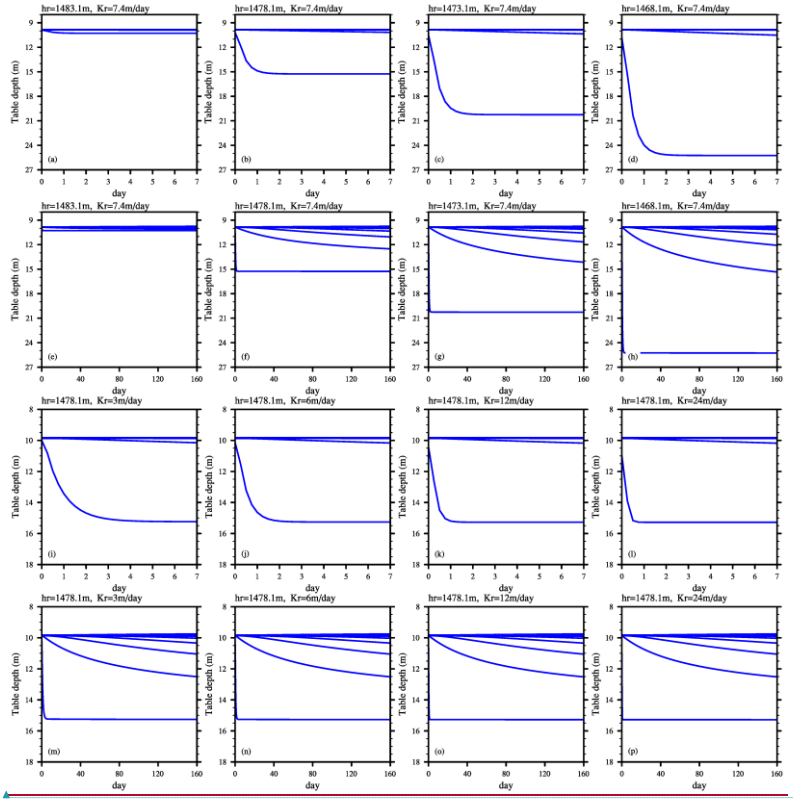

带格式的：字体：Times New Roman，10 磅

带格式的：居中

带格式的：居中，定义网格后不调整右缩进，行距：2 倍行距，无孤行控制，取消行号，不调整西文与中文之间的空格，不调整中文和数字之间的空格

Figure 54 (a-d, i-l) Short-term and (e-h, m-p) long-term responses of riparian groundwater table to the river water level h_r and river bed hydraulic conductivity K_r in the case of– groundwater recharge river~~river recharging groundwater~~. (a-h) Time series of the simulated groundwater table depths for each grid cell in the first sensitivity experiment. (i-p) Time series for the second sensitivity experiment.

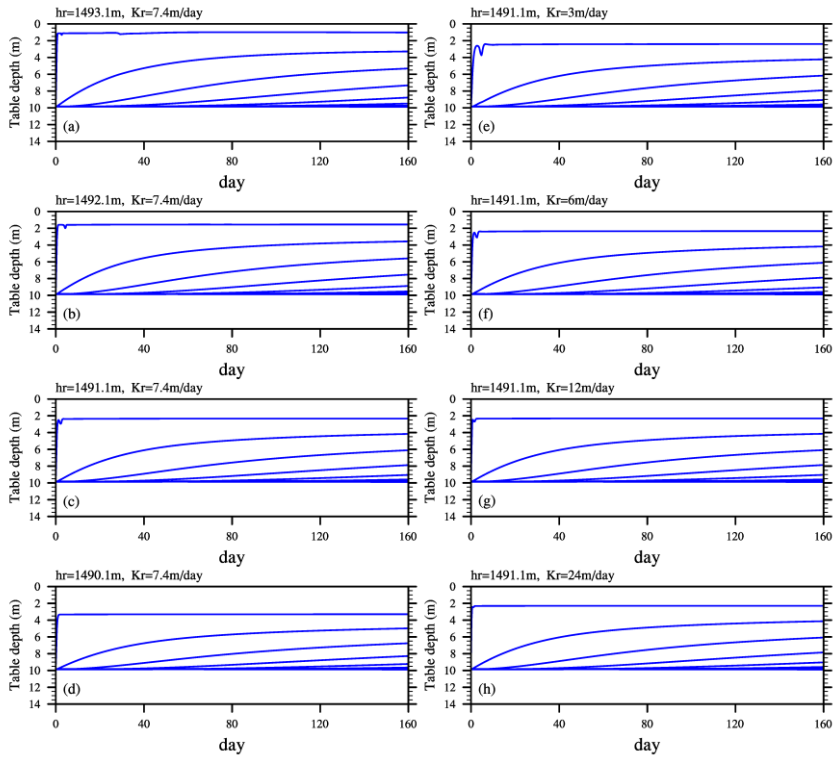

~~**Figure 5** Long-term (in 160 days) responses of riparian groundwater table to the river water level h_r~~

带格式的：字体：Times New Roman，10 磅

带格式的：居中

and river bed hydraulic conductivity K_r in the situation of river recharging groundwater. (a-d) Time series of the simulated groundwater table depths for each grid cell in the first sensitivity experiment. (e-h) Time series for the second sensitivity experiment.

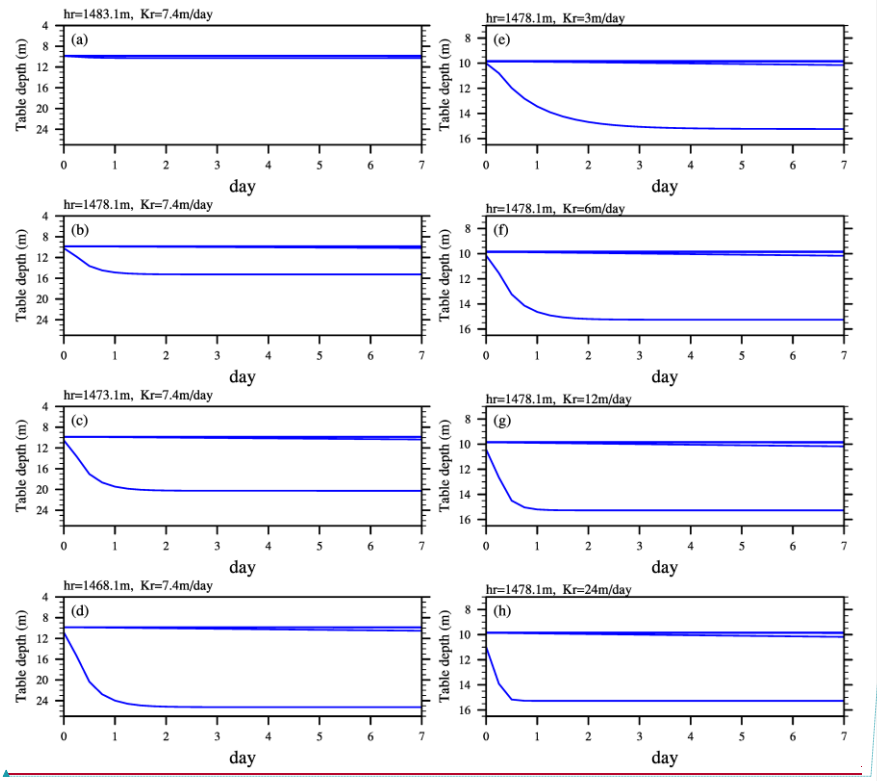

Figure 6 Short-term (in 7 days) responses of riparian groundwater table to the river water level h_c and river bed hydraulic conductivity K_c in the situation of groundwater recharging river. (a-d) Time series of the simulated groundwater table depths for each grid cell in the first sensitivity experiment. (e-h) Time series for the second sensitivity experiment.

带格式的： 字体：Times New Roman，10 磅

带格式的： 左，定义网格后自动调整右缩进，行距：单倍行距，孤行控制，不取消行号，调整中文与西文文字的间距，调整中文与数字的间距

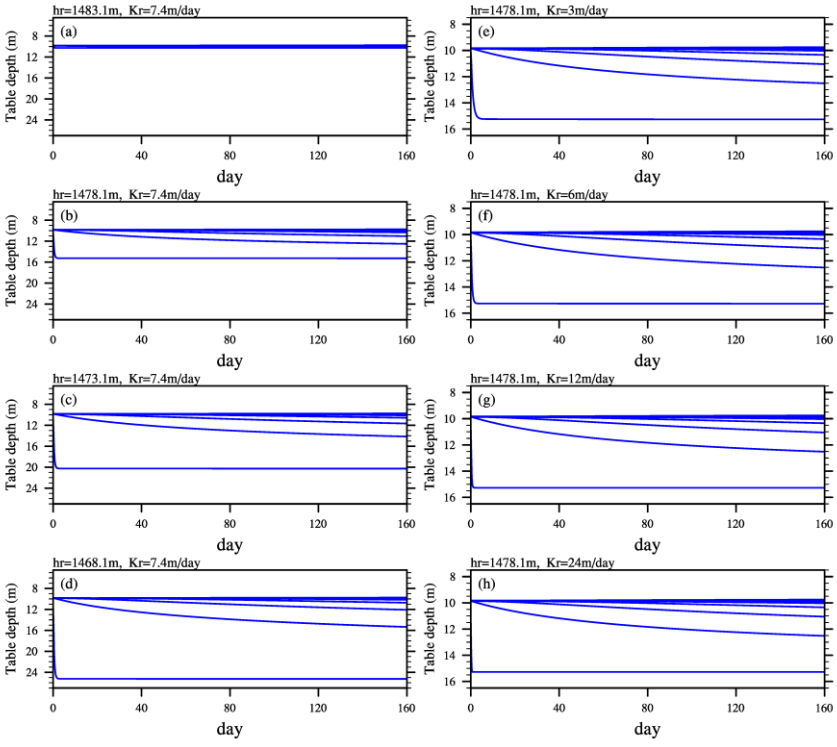

Figure 7 Long-term (in 160 days) responses of riparian groundwater table to the river water level h_r and river bed hydraulic conductivity K_r in the situation of groundwater recharging river. (a-d) Time series of the simulated groundwater table depths for each grid cell in the first sensitivity experiment. (e-h) Time series for the second sensitivity experiment.

带格式的：字体：Times New Roman，10 磅

带格式的：左，定义网格后自动调整右缩进，行距：单倍行距，孤行控制，不取消行号，调整中文与西文文字的间距，调整中文与数字的间距

带格式的：居中

带格式的：左，定义网格后自动调整右缩进，行距：单倍行距，孤行控制，不取消行号，调整中文与西文文字的间距，调整中文与数字的间距

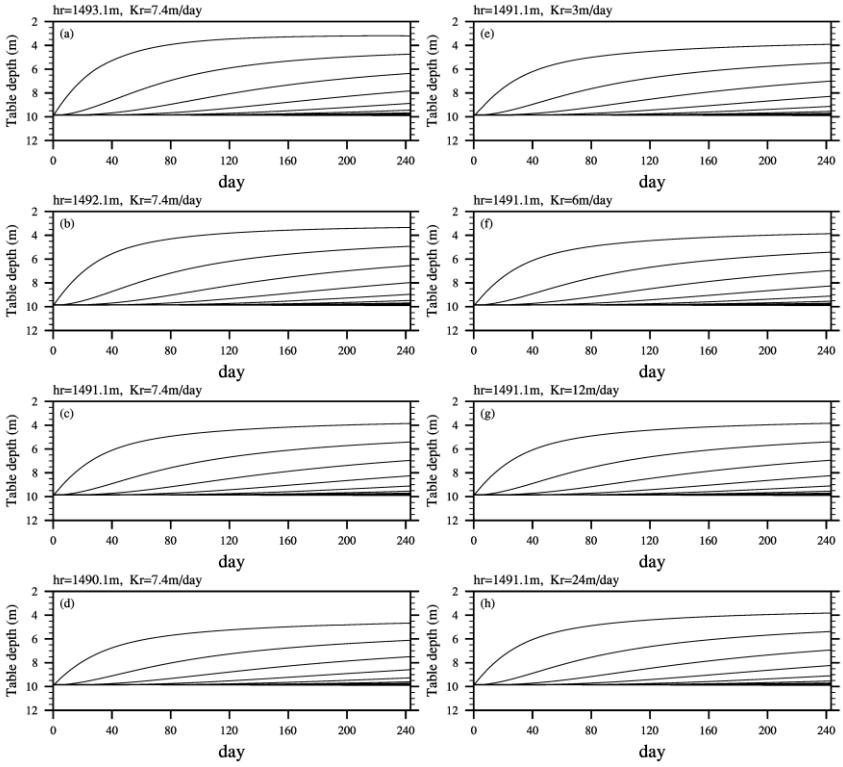

Figure 4 Sensitivities of the river water level hr and river bed hydraulic conductivity Kr. (a–d) Time series of the simulated groundwater table depths for 20 grid cells in the first sensitivity experiment. (e–h) Time series for the second sensitivity experiment.

带格式的： 字体：（默认）Times New Roman，（中文）Times New Roman，10 磅

带格式的： 居中，定义网格后自动调整右缩进，段落间距段前：12 磅，段后：12 磅，调整中文与西文文字的间距，调整中文与数字的间距

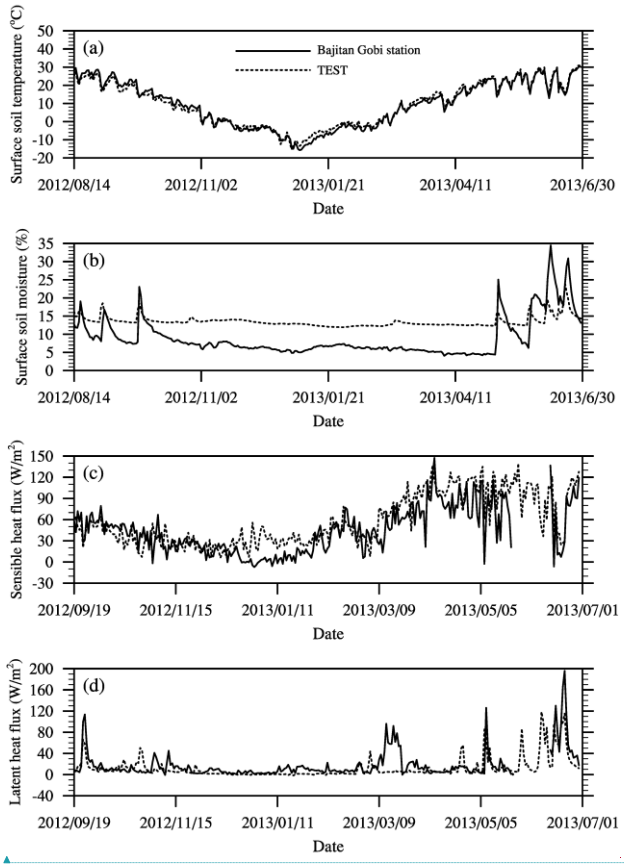

带格式的： 字体：(默认) Times New Roman, (中文) Times New Roman, 10 磅

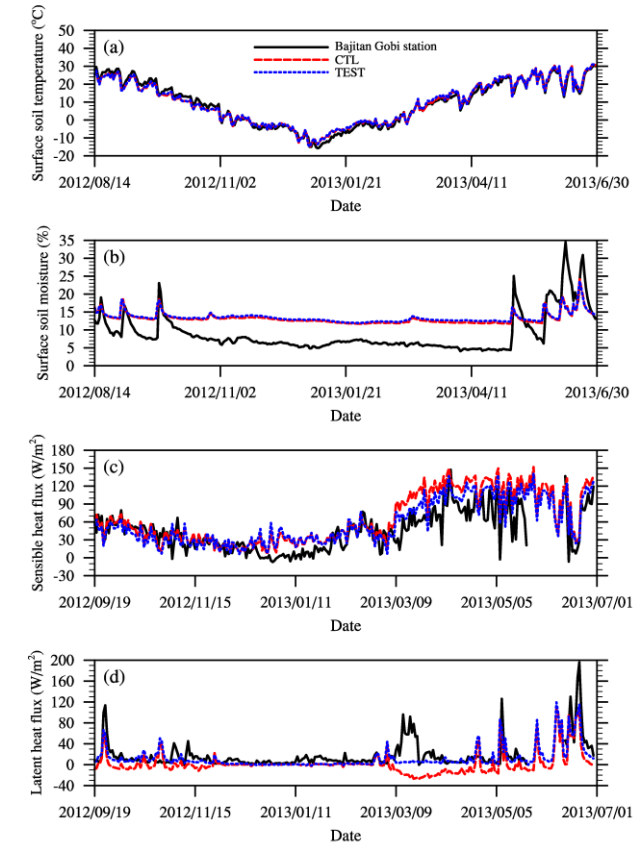

Figure ~~6~~5 Time series of the observations from the eddy covariance and automatic weather station systems and results from the CTL and TEST simulations at Bajitan Gobi station for (a) surface soil temperature, (b) surface soil moisture, (c) sensible heat flux and (d) latent heat flux.

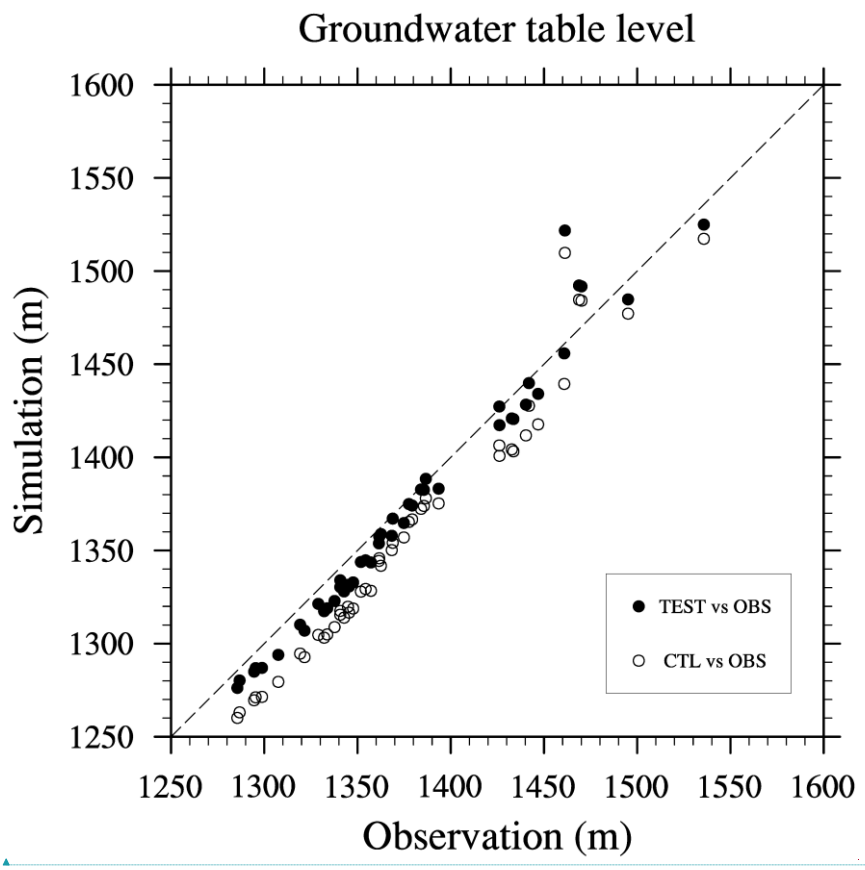

带格式的： 字体：(默认) Times New Roman, (中文) Times New Roman, 10 磅

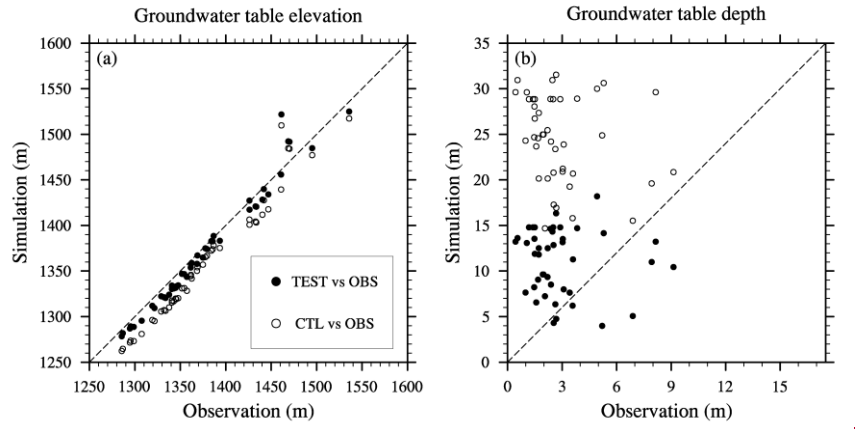
Groundwater table elevation
(a)
Simulation (m)
Observation (m)
TEST vs OBS
CTL vs OBS
Groundwater table depth
(b)
Simulation (m)
Observation (m)

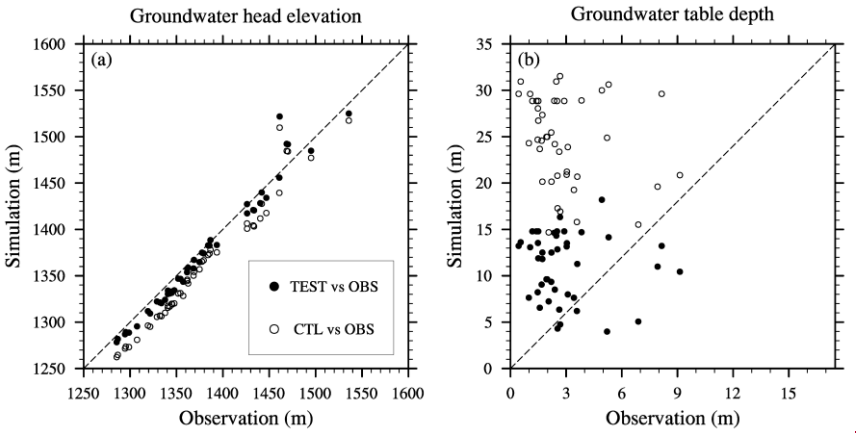
Groundwater head elevation
(a)
Simulation (m)
Observation (m)
TEST vs OBS
CTL vs OBS
Groundwater table depth
(b)
Simulation (m)
Observation (m)

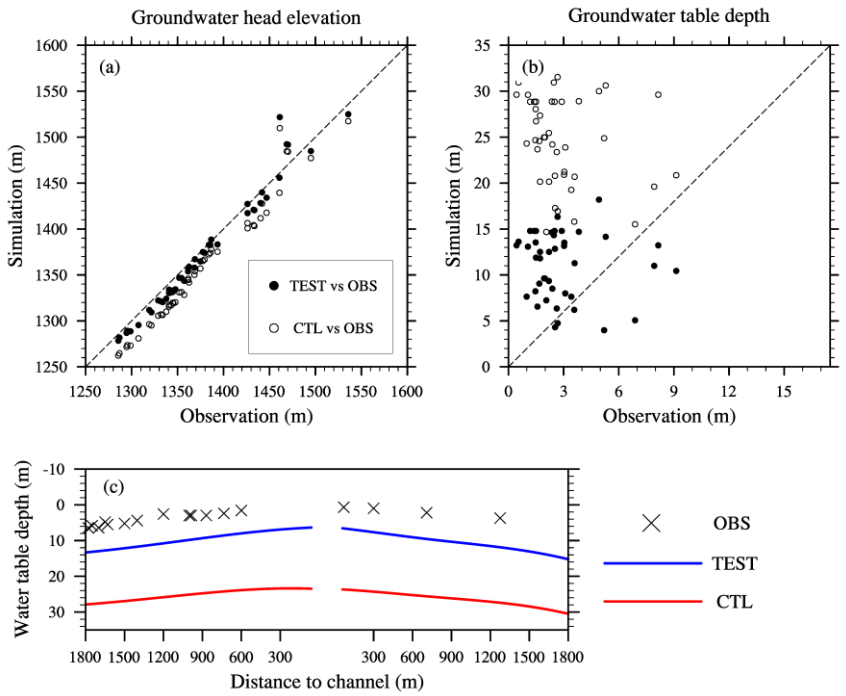

Figure 7~~6~~ (a) Annual groundwater head ~~table~~ elevation~~head~~, ~~and~~ (b) groundwater table depth predicted by TEST and CTL simulations against observed climatology water head data from 46 observation wells and~~.~~ (c) spatial distribution of groundwater table depth from observation, TEST and CTL over the Gaotai Bridge.

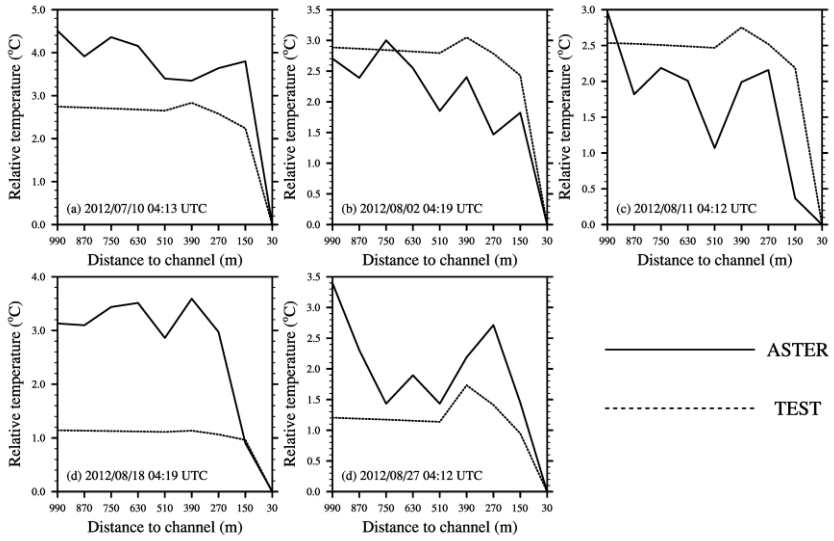

带格式的：字体：（默认）Times New Roman，（中文）Times New Roman，10 磅

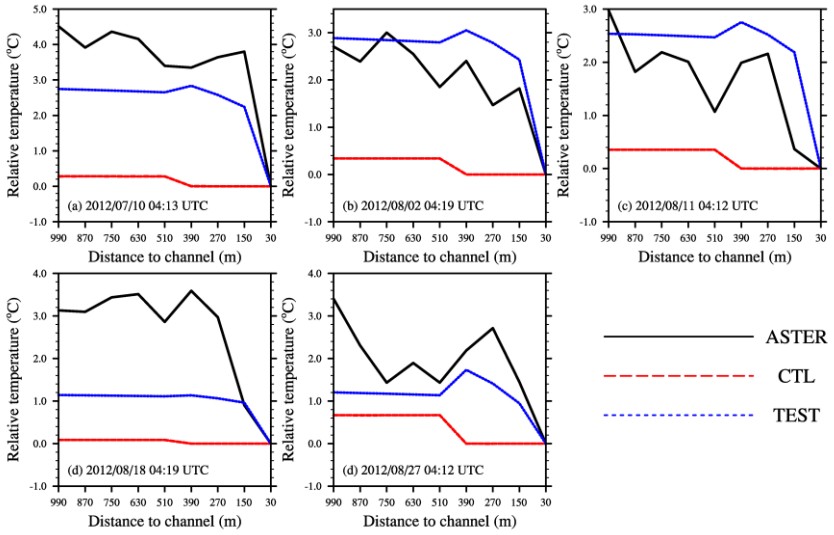
Relative temperature (°C)
(a) 2012/07/10 04:13 UTC
(b) 2012/08/02 04:19 UTC
(c) 2012/08/11 04:12 UTC
(d) 2012/08/18 04:19 UTC
(d) 2012/08/27 04:12 UTC
990 870 750 630 510 390 270 150 30
Distance to channel (m)
ASTER
CTL
TEST

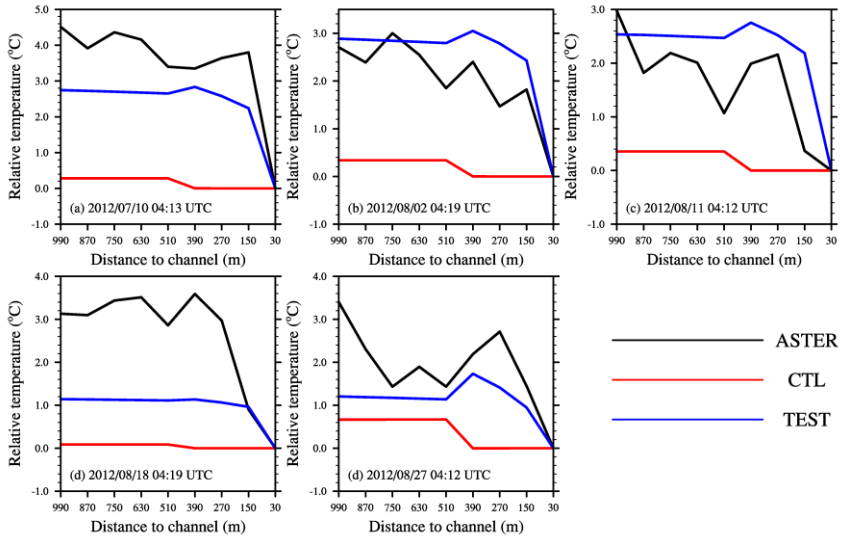

Figure ~~8~~7 Relative ground temperature across the left riverbank of the 213 Bridge station from the CTL and TEST simulations and corresponding remote sensing data from five ASTER satellite transit events of (a) 2012/07/10 04:13 UTC, (b) 2012/08/02 04:19 UTC, (c) 2012/08/11 04:12 UTC, (d) 2012/0818 04:19 UTC and (e) 2012/08/27 04:12 UTC.

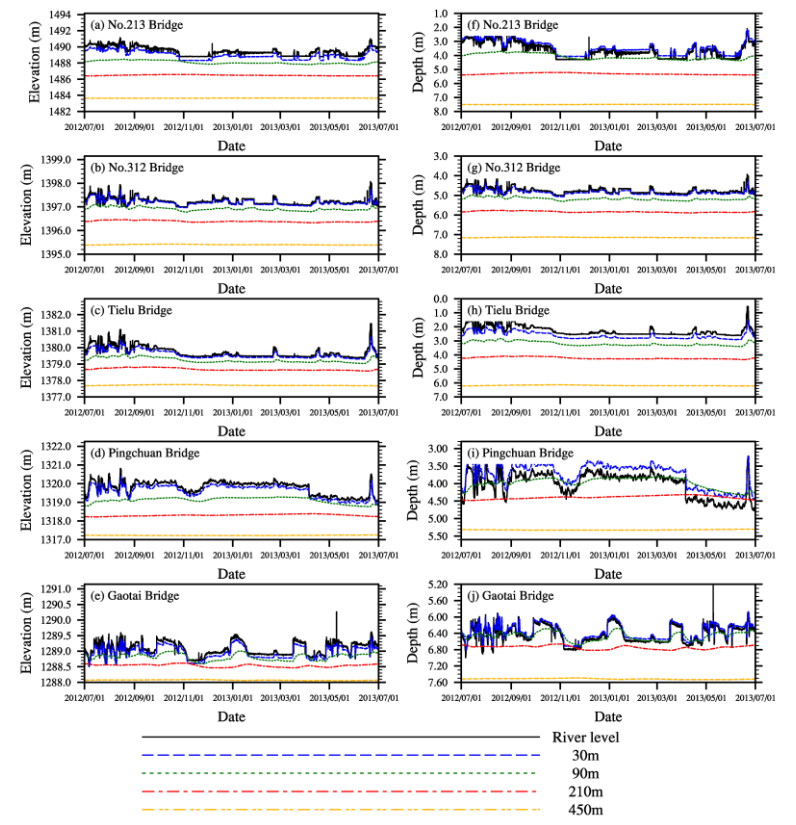

带格式的：字体：Times New Roman，10 磅

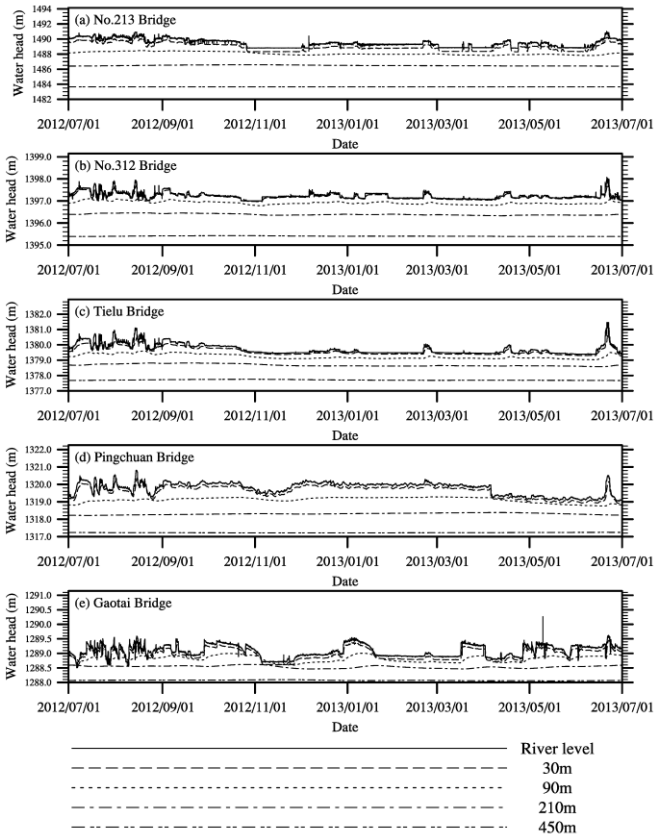
(a) No.213 Bridge
Water head (m)
1494
1492
1490
1488
1486
1484
1482
2012/07/01
2012/09/01
2012/11/01
2013/01/01
2013/03/01
2013/05/01
2013/07/01
Date
(b) No.312 Bridge
Water head (m)
1399.0
1398.0
1397.0
1396.0
1395.0
Date
(c) Tielu Bridge
Water head (m)
1382.0
1381.0
1380.0
1379.0
1378.0
1377.0
Date
(d) Pingchuan Bridge
Water head (m)
1322.0
1321.0
1320.0
1319.0
1318.0
1317.0
Date
(e) Gaotai Bridge
Water head (m)
1291.0
1290.5
1290.0
1289.5
1289.0
1288.5
1288.0
Date
River level
30m
90m
210m
450m

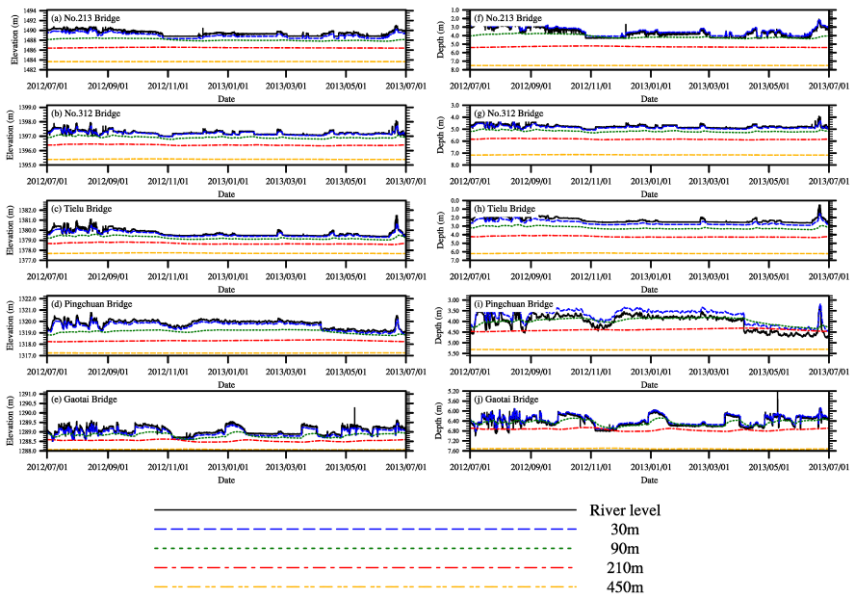

Figure ~~9~~8 Time series of simulated (a-e) water head elevations and (f-j) water table depthss at 30 m, 90 m, 210 m and 450 m from streams and the observed river water levels at the five left riverbanks of stations at (a, f) 213 Bridge, (b, g) 312 Bridge, (c, h) Tielu Bridge, (d, i) Pingchuan Bridge and (e, j) Gaotai Bridge.

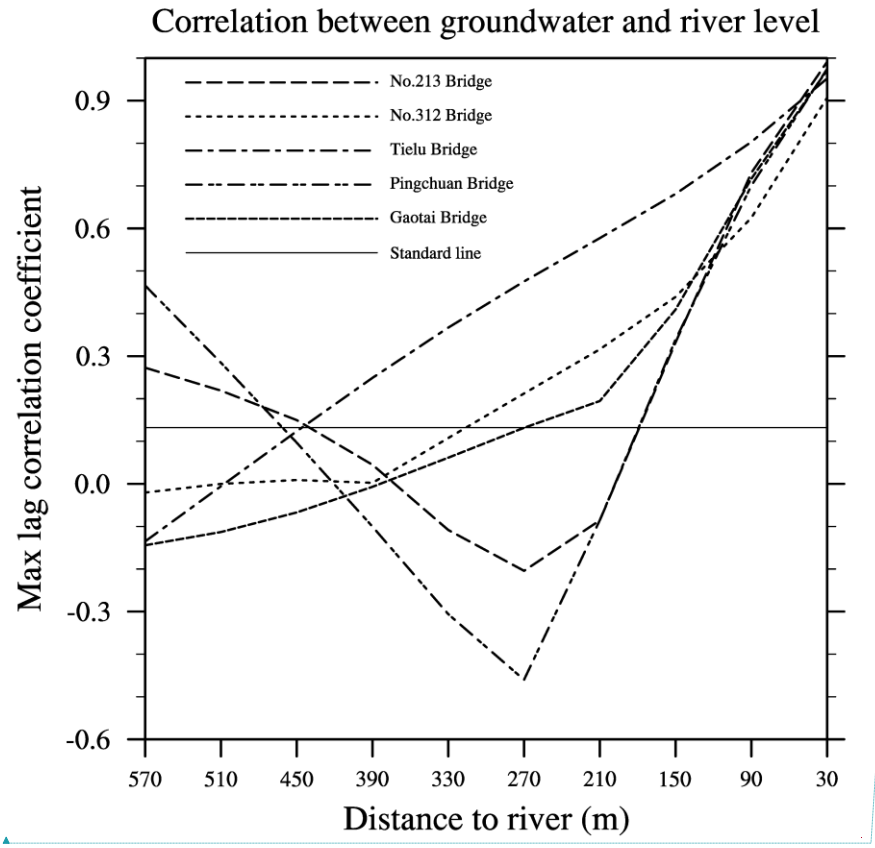

带格式的: 字体: Times New Roman, 10 磅

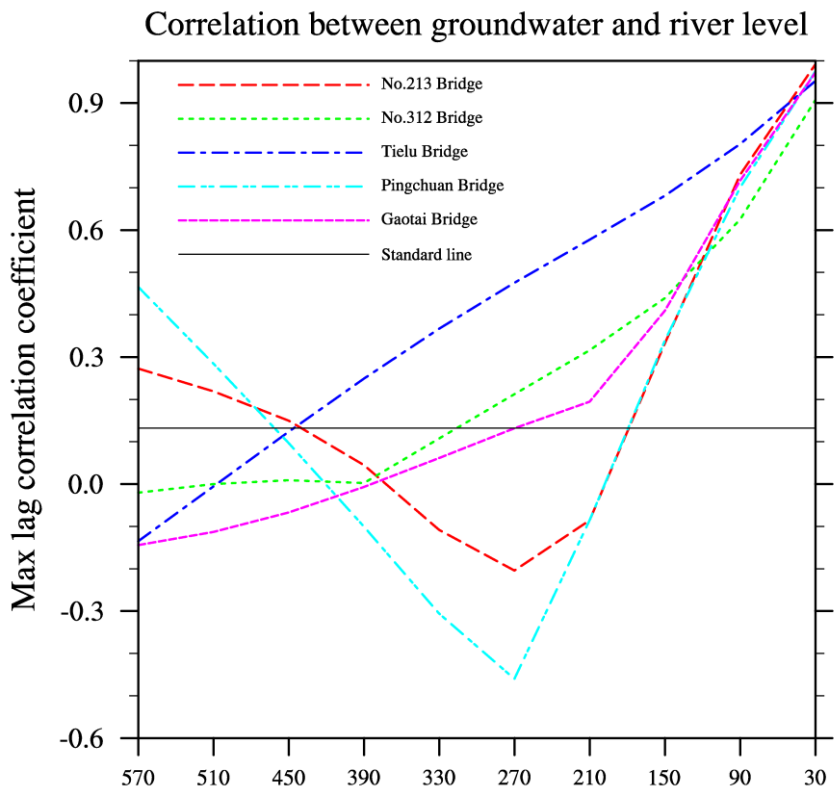

Figure 10~~9~~ Maximum lag correlation coefficients between simulated groundwater tables across the left riverbanks and the river water levels at the five stations, and the standard line representing the value of correlation coefficient passing the Student's t test with a confidence level of 95%.

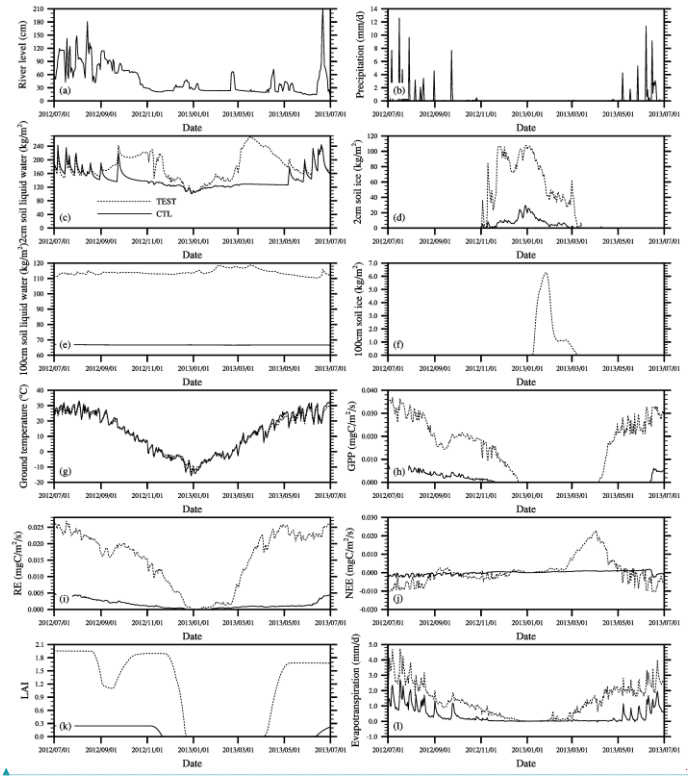

带格式的：字体：Times New Roman，10 磅

带格式的：两端对齐

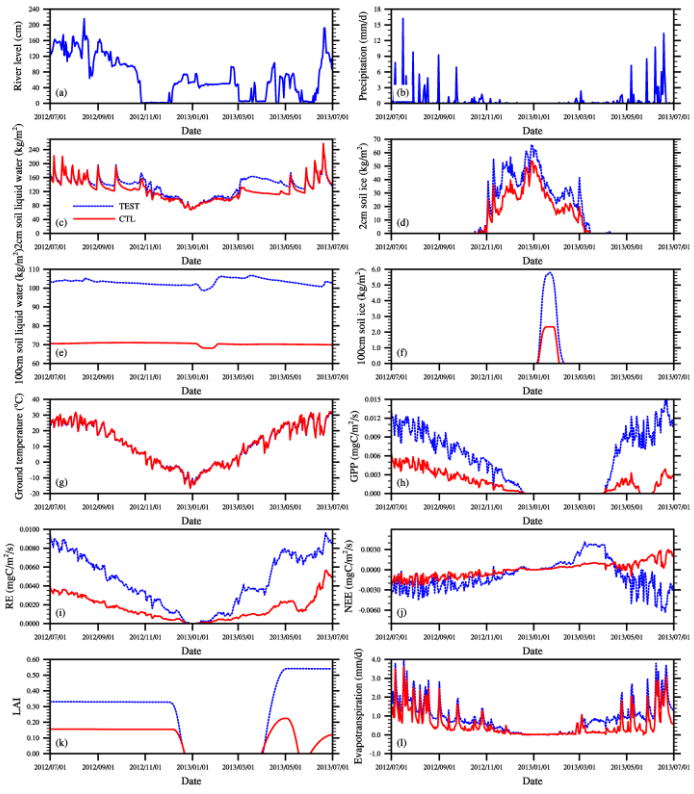
River level (cm)
(a)
Precipitation (mm/d)
(b)
Date
2cm soil liquid water (kg/m²)
TEST
CTL
(c)
2cm soil ice (kg/m²)
(d)
100cm soil liquid water (kg/m²)
(e)
100cm soil ice (kg/m²)
(f)
Ground temperature (°C)
(g)
GPP (mgC/m²/s)
(h)
RE (mgC/m²/s)
(i)
NEE (mgC/m²/s)
(j)
LAI
(k)
Evapotranspiration (mm/d)
(l)

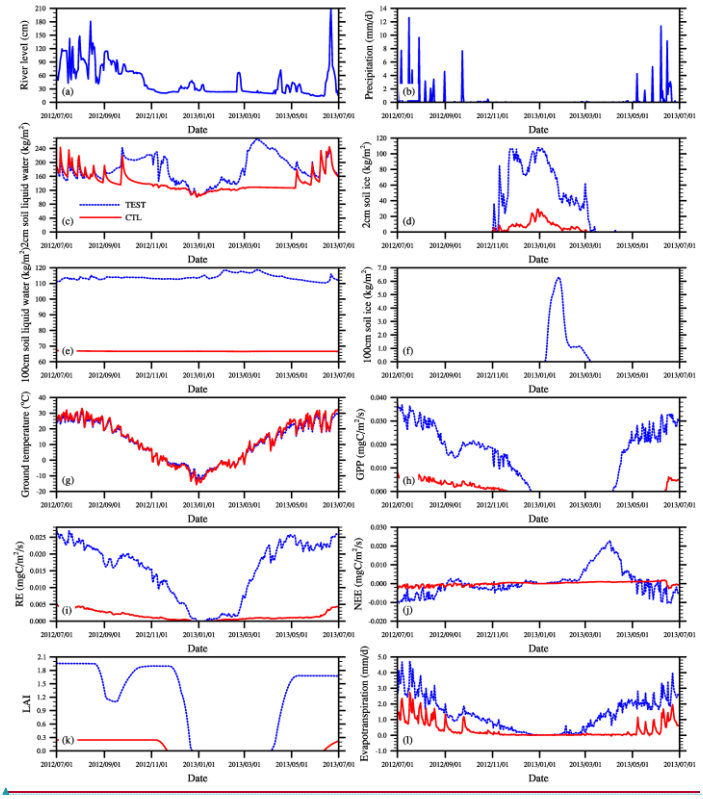

Figure 1~~0~~1 Time series of area-averaged daily (a) observed river level and (b) observed precipitation, as well as (c) 2-cm soil liquid water, (d) 2-cm soil ice, (e) 100-cm soil liquid water, (f) 100-cm soil ice, (g) ground temperature, (h) gross primary productivity, (i) respiration efficiency, (j) net ecosystem exchange, (k) leaf area index and (l) evapotranspiration predicted by TEST and CTL simulations within 300 m of both sides of the stream at the Tielu Bridge station.

带格式的: 字体: Times New Roman, 10 磅

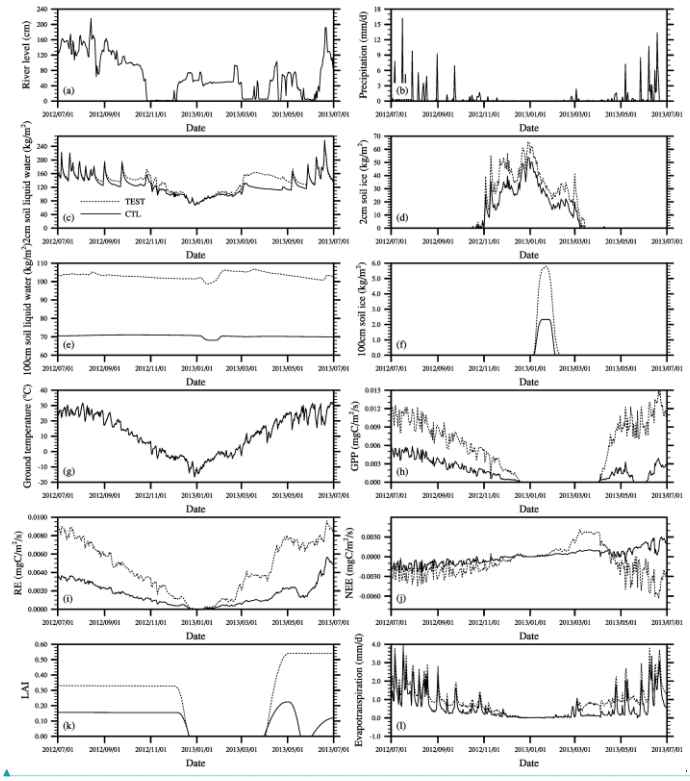

带格式的：字体：Times New Roman，10 磅

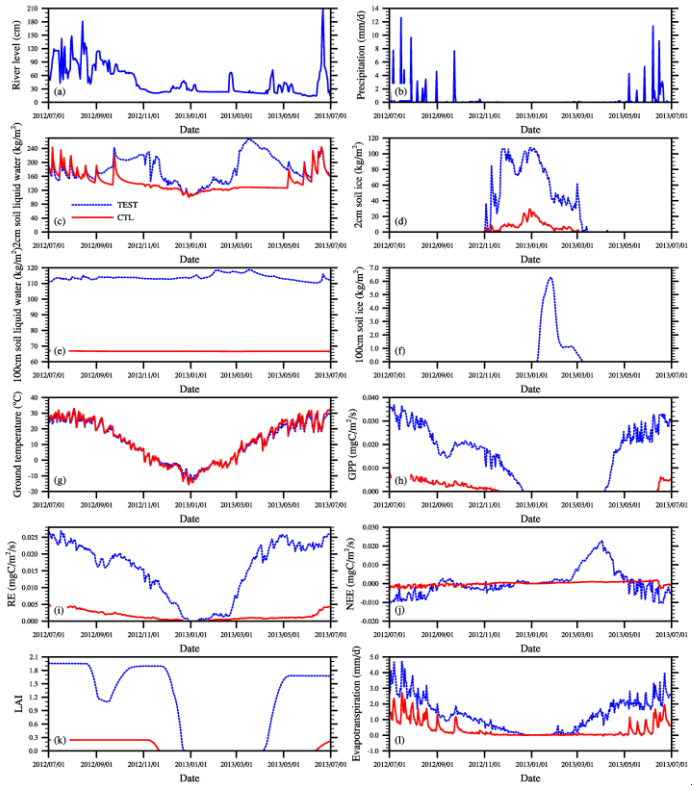
River level (cm)
Precipitation (mm/d)
2cm soil liquid water (kg/m²)
2cm soil ice (kg/m³)
100cm soil liquid water (kg/m²)
100cm soil ice (kg/m³)
Ground temperature (°C)
GPP (mgC/m²/s)
RE (mgC/m²/s)
NEE (mgC/m²/s)
LAI
Evapotranspiration (mm/d)
Date
TEST
CTL
(a)
(b)
(c)
(d)
(e)
(f)
(g)
(h)
(i)
(j)
(k)
(l)

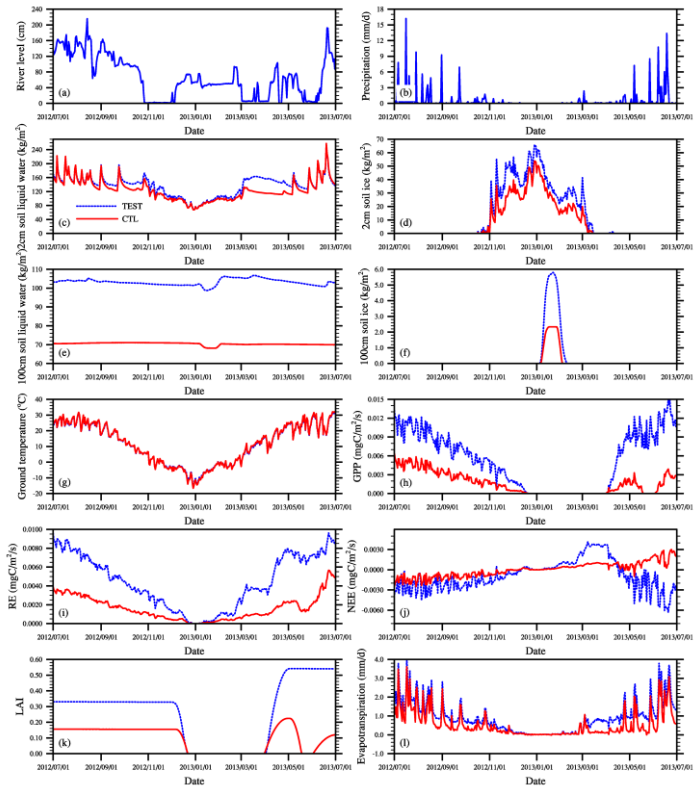

Figure 1~~2~~1 Time series of area-averaged daily (a) observed river level and (b) observed precipitation, as well as (c) 2-cm soil liquid water, (d) 2-cm soil ice, (e) 100-cm soil liquid water, (f) 100-cm soil ice, (g) ground temperature, (h) gross primary productivity, (i) respiration efficiency, (j) net ecosystem

exchange, (k) leaf area index and (l) evapotranspiration predicted by TEST and CTL simulations within 300 m of both sides of the stream at the 213 Bridge station.

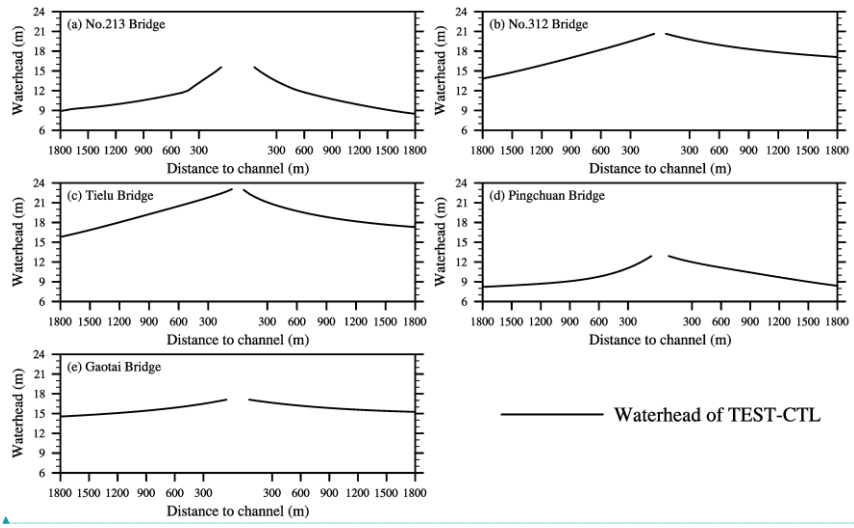

带格式的：字体：Times New Roman，10 磅

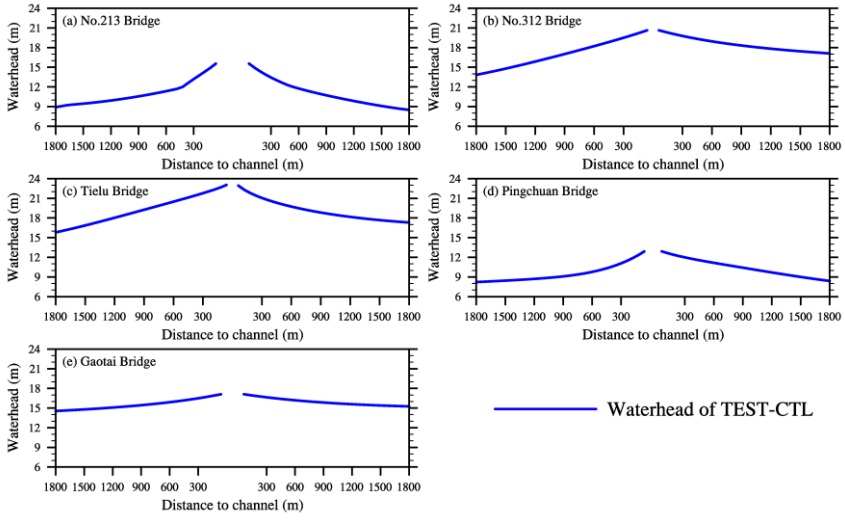
(a) No.213 Bridge
(b) No.312 Bridge
(c) Tielu Bridge
(d) Pingchuan Bridge
(e) Gaotai Bridge
Waterhead (m)
Distance to channel (m)
1800 1500 1200 900 600 300 300 600 900 1200 1500 1800
Waterhead of TEST-CTL

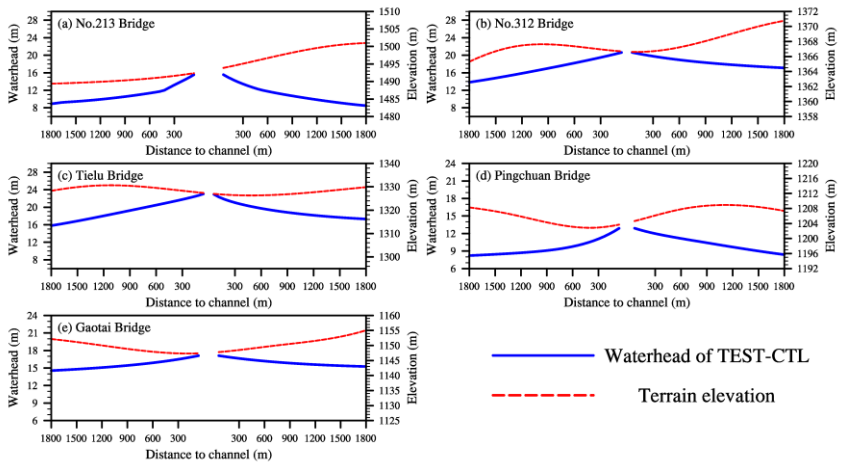
(a) No.213 Bridge
(b) No.312 Bridge
(c) Tielu Bridge
(d) Pingchuan Bridge
(e) Gaotai Bridge
Waterhead (m)
Elevation (m)
Distance to channel (m)
1800 1500 1200 900 600 300 300 600 900 1200 1500 1800
Waterhead of TEST-CTL
Terrain elevation

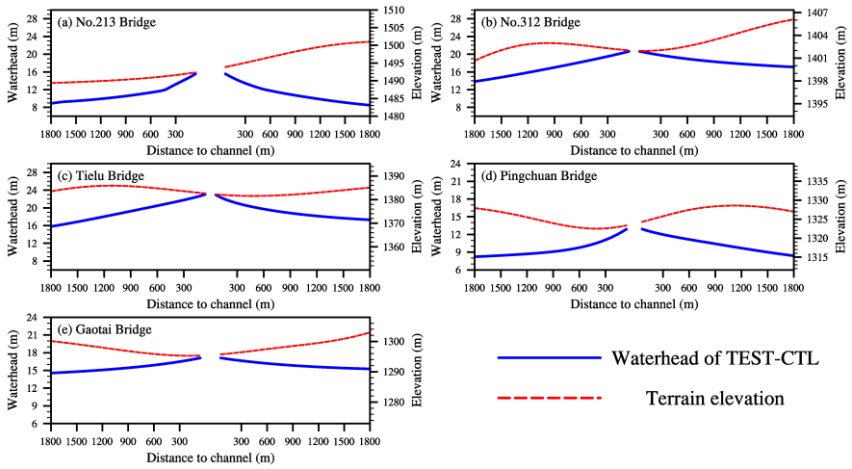

Figure 13~~2~~ Differences between annual water heads predicted by TEST and CTL simulations and terrain elevations along the five sections at (a) 213 Bridge, (b) 312 Bridge, (c) Tielu Bridge, (d) Pingchuan Bridge and (e) Gaotai Bridge. The discontinuous parts of the curves represent the river areas.

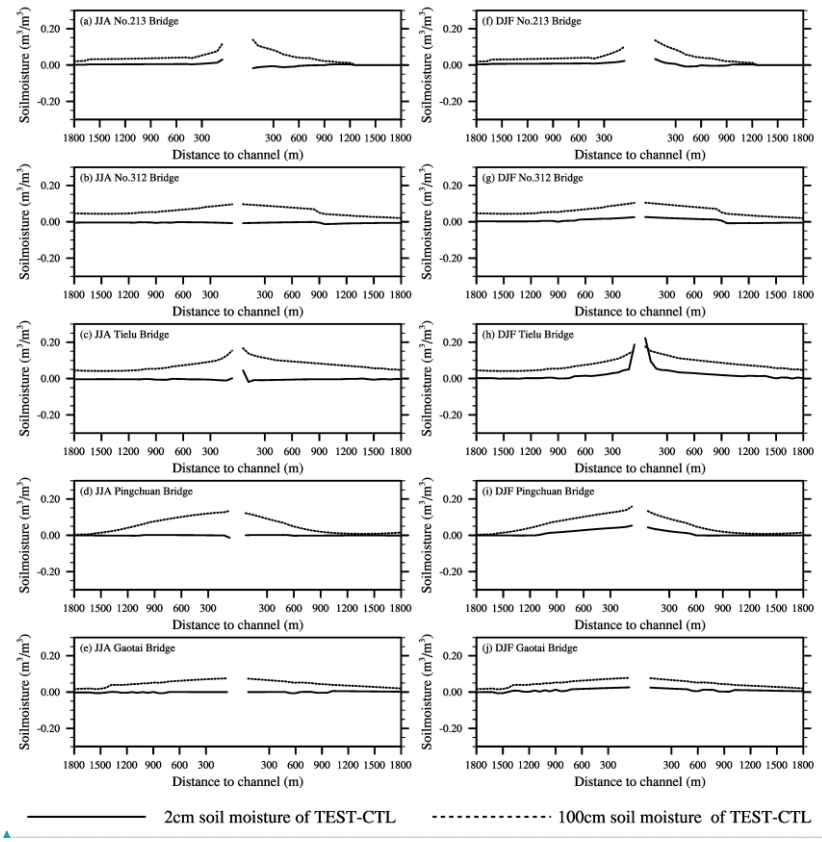

带格式的：字体：Times New Roman，10 磅

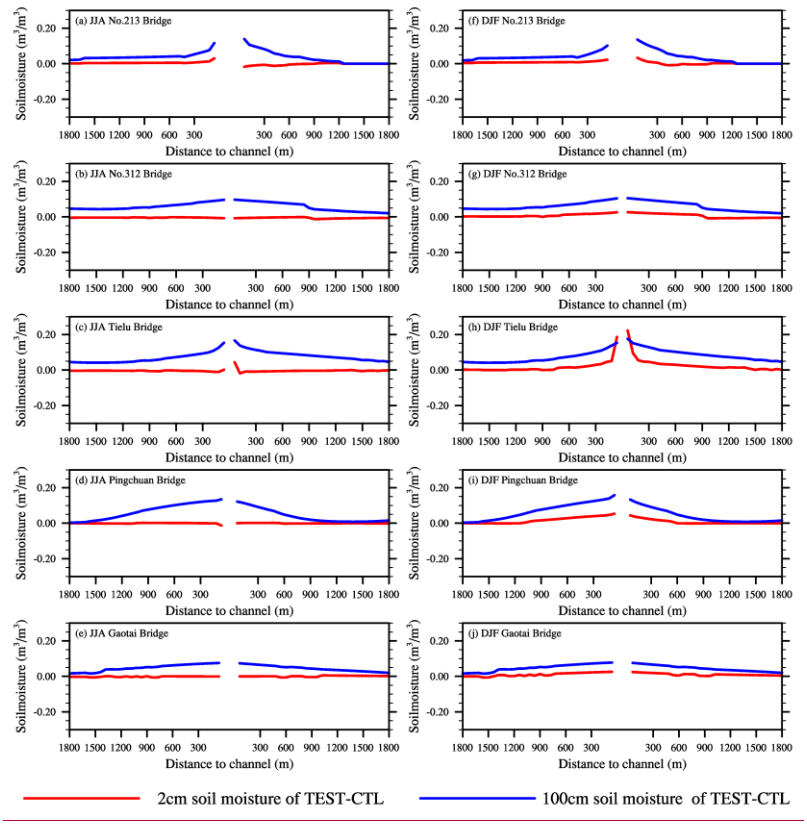

Figure 1~~2~~3 Differences of (a–e) summer and (f–j) winter soil moisture (both liquid water and ice are included) predicted at depths of 2 cm and 100 cm by TEST and CTL simulations along the five sections at (a and f) 213 Bridge, (b and g) 312 Bridge, (c and h) Tielu Bridge, (d and i) Pingchuan Bridge and (e and j) Gaotai Bridge. The discontinuous parts of the curves represent the river areas.

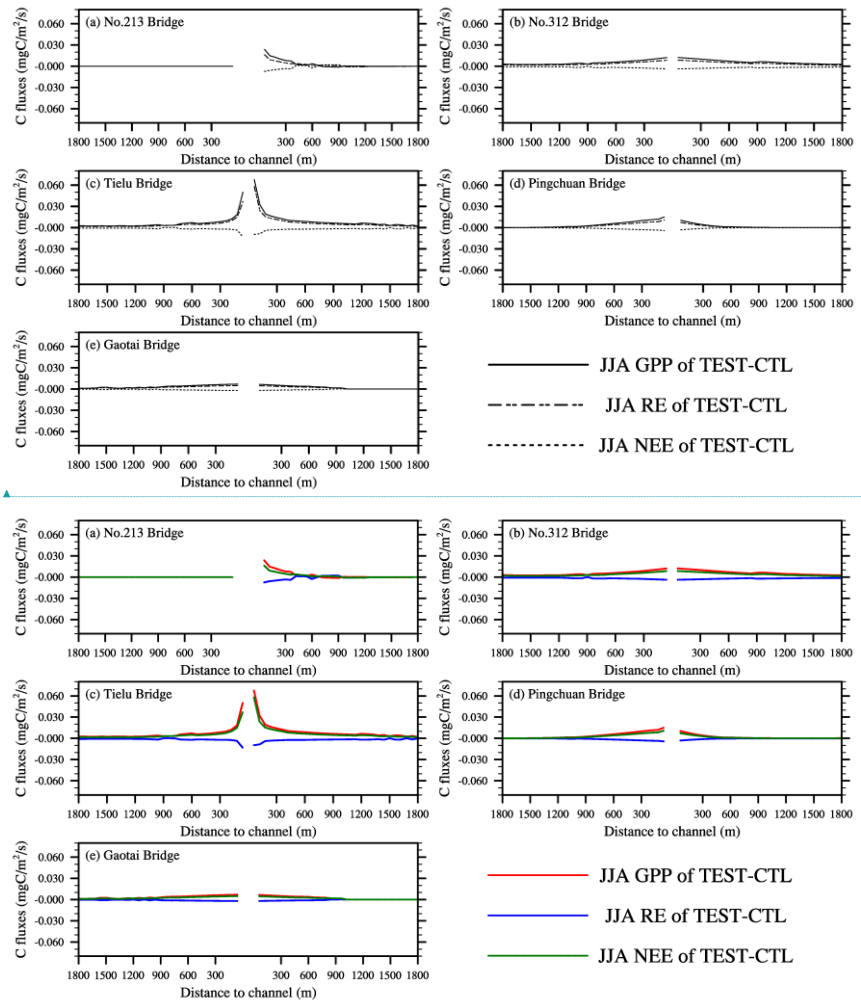

Figure 1~~5~~4. Differences between gross primary productivity, respiration efficiency and net ecosystem

带格式的： 字体: Times New Roman, 10 磅

exchange predicted by TEST and CTL simulations during summer along the five sections at (a) 213 Bridge, (b) 312 Bridge, (c) Tielu Bridge, (d) Pingchuan Bridge and (e) Gaotai Bridge. The discontinuous parts of the curves represent the river areas.

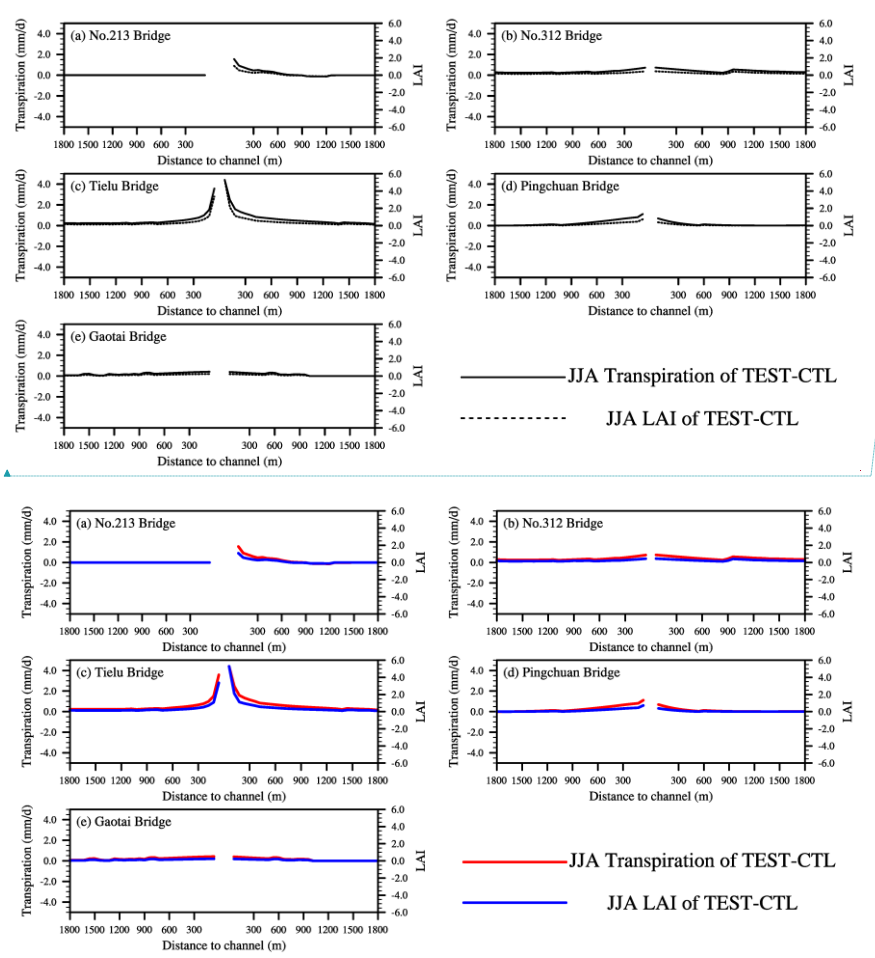

Figure 1~~6~~5. Differences between canopy transpiration and leaf area index predicted by TEST and CTL simulations during summer along the five sections at (a) 213 Bridge, (b) 312 Bridge, (c) Tielu Bridge,

带格式的：字体：Times New Roman，10 磅

(d) Pingchuan Bridge and (e) Gaotai Bridge. The discontinuous parts of the curves represent the river areas.

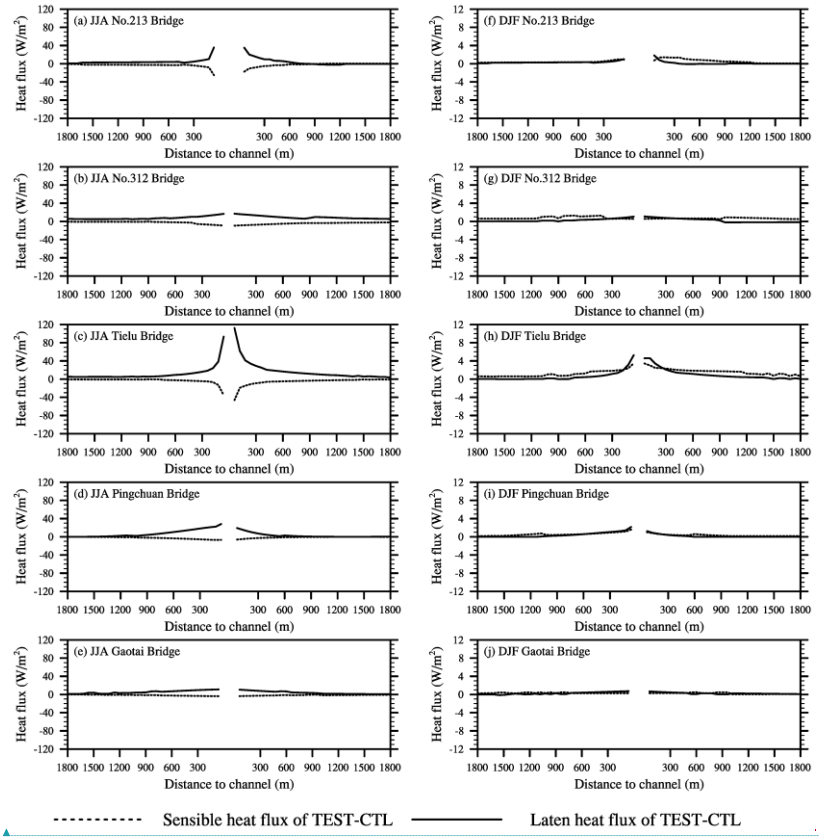

带格式的：字体：Times New Roman，10 磅

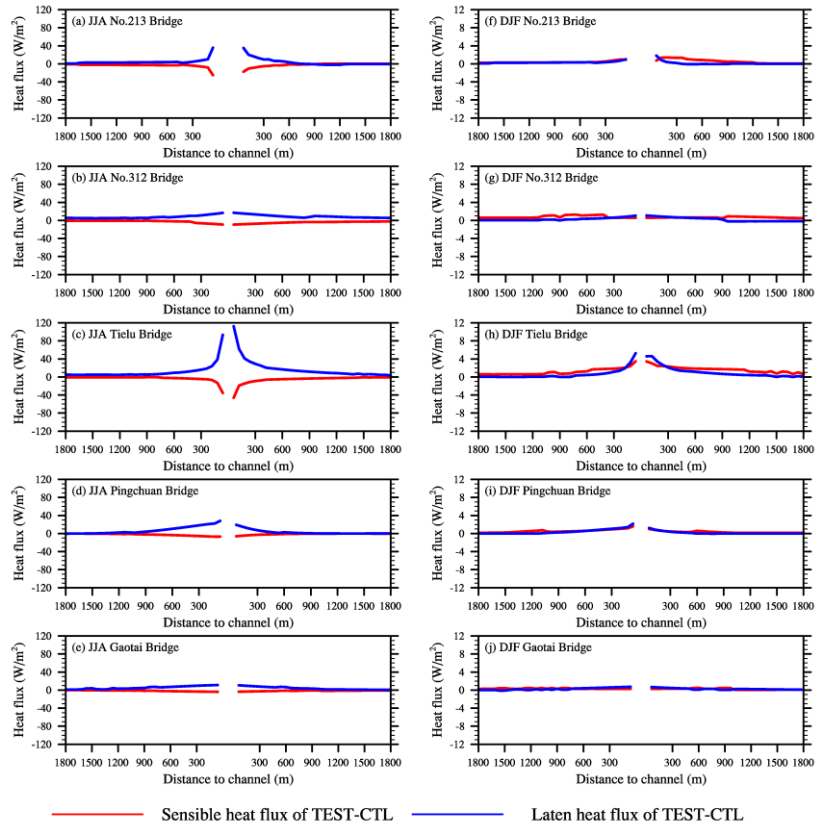

Figure 1~~7~~6 Differences of (a–e) sensible and (f–j) latent heat fluxes predicted by TEST and CTL simulations along the five sections at (a and f) 213 Bridge, (b and g) 312 Bridge, (c and h) Tielu Bridge, (d and i) Pingchuan Bridge and (e and j) Gaotai Bridge. The discontinuous parts of the curves represent the river areas.